Age structure eliminates the impact of coinfection on epidemic dynamics in a freshwater zooplankton system

Patrick A. Clay^{1,a}, Sabrina Gattis^{2,b}, Jade Garcia¹, Vincent Hernandez¹, Frida Ben-Ami^{2,c},

Meghan A. Duffy^{1,d}

¹Department of Ecology & Evolutionary Biology, University of Michigan

²School of Zoology, George S. Wise Faculty of Life Sciences, Tel Aviv University, Tel Aviv 6997801, Israel;

^aORCID: 0000-0002-8142-0802

^bORCID: 0000-0002-2460-8243

^cORCID: 0000-0002-1978-5659

^dORCID: 0000-0002-8142-0802

Keywords: Host, Parasite, Age, Coinfection, Freshwater, Zooplankton

MS type: Article

Abstract

Parasites often coinfect host populations, and, by interacting within hosts, might change the trajectory of multi-parasite epidemics. However, host-parasite interactions often change with host age, raising the possibility that within-host interactions between parasites might also change, influencing the spread of disease. We measured how heterospecific parasites interacted within zooplankton hosts and how host age changed these interactions. We then parameterized an epidemiological model to explore how age-effects altered the impact of coinfection on epidemic dynamics. In our model, we found that in populations where epidemiologically relevant parameters did not change with age, the presence of a second parasite altered epidemic dynamics. In contrast, when parameters varied with host age (based on our empirical measures), there was no longer a difference in epidemic dynamics between singly and coinfected populations, indicating that variable age structure within a population eliminates the impact of coinfection on epidemic dynamics. Moreover, infection prevalence of both parasites was lower in populations where epidemiologically relevant parameters changed with age. Given that hostpopulation age structure changes over time and space, these results indicate that age-effects are important for understanding epidemiological processes in coinfected systems and that studies focused on a single age group could yield inaccurate insights.

Introduction

Parasites that infect the same host population interact with one another, and ultimately alter one another's epidemic dynamics (Abu-Raddad *et al.* 2008). At the host population scale, parasites interact by altering the availability and susceptibility of potential hosts (Ezenwa *et al.* 2010). For instance, measles may interfere with whooping cough transmission by killing susceptible hosts, and vice versa (Rohani *et al.* 2003). At the within-host scale, parasites interact by altering each other's within-host growth rates, the duration of infection, and virulent effects on the host (Ben-Ami *et al.* 2011; Duncan *et al.* 2015; Ezenwa & Jolles 2015). For instance, malaria infection can increase HIV viral load, and thus HIV transmissibility (Abu-Raddad *et al.* 2006).

Interactions among parasites change as hosts age (Izhar *et al.* 2015). Interactions between parasites infecting the same host change with host age because of host physiology (including changes in body size, nutritional status, and immune function) and behavior (reviewed in Ben-Ami 2019). Host immune systems typically grow stronger as hosts age, before becoming weaker late in life (Hamilton 1966; Simon *et al.* 2015). Shifting immune strength as hosts age will shift immune-based parasite interactions, such as immune-suppression and cross-immunity, that determine host susceptibility, the growth rate of parasites within hosts, and host mortality (Raberg *et al.* 2006; Ezenwa & Jolles 2015; Halliday *et al.* 2020; Clark *et al.* 2021).

Additionally, many within-host interactions are based on resources within the host. As hosts age, their resource consumption typically increases, and the proportion of resources they direct towards growth, somatic maintenance, immune function, and reproduction shift (Forseth *et al.* 1994; Demott *et al.* 2010) — likely changing the strength of resource competition between parasites. Further, parasites can change the foraging behavior of hosts (Karban & English-Loeb

1997; Penczykowski *et al.* 2022) and their predators (Goren & Ben-Ami 2017), and thus the rate at which hosts come in contact with secondary parasites. However, the strength of this behavioral manipulation can also depend on age (Poulin 1993). Thus, there are a variety of mechanisms that could shift parasite interactions over a host's lifespan.

While we know host age can alter parasite interactions at the individual scale, limited research has been done on how these age-effects scale up to alter multi-parasite epidemic dynamics at the population scale (reviewed in Ben-Ami 2019). In single-parasite systems, individual-level age-effects can scale up to influence epidemic dynamics (Ben-Ami 2019; Clark et al. 2021). Explicitly modelling age-effects has improved our ability to predict and respond to epidemics of virulent childhood diseases such as whooping cough and measles (Finkenstädt & Grenfell 2000), and thus could improve our ability to predict dynamics of multi-parasite systems. We expect age-effects to scale up to alter disease dynamics in multi-parasite systems via agemediated feedback loops (Fig. 1). Through these feedback loops, parasite interactions increase (or decrease) transmission, which decreases (or increases) the average age at which hosts become infected (Anderson & May 1985), altering the strength of parasite interactions and further influencing transmission. Given that epidemiological feedback loops can fundamentally alter disease processes (Fenton et al. 2008; Clay et al. 2020), we expect that multi-parasite models that incorporate age-effects will make systematically different predictions than models that do not.

We used a system of freshwater zooplankton coinfected by fungal and bacterial parasites to ask (1) how does host age alter interactions between parasites? and (2) how do age-effects in individual hosts scale up to alter epidemics in the host population? To answer these questions, we measured host lifespan, reproduction, contact with parasites, susceptibility, and infectious

propagule production in zooplankton singly infected and co-infected by fungal and bacterial spores, and used these measurements to parameterize an agent-based epidemic model. Overall, our results indicate that host age can mediate the strength of within-host interactions, and that variation in parasite interactions with host age can decrease infection prevalence in our system. Most interestingly, when epidemiologically relevant parameters (feeding rate, per-spore susceptibility, spore yield, and births per day) were allowed to vary with host age, as measured in our laboratory study, differences in epidemic dynamics between singly- and co-infected populations were eliminated.

Empirical Methods

Study System

We used *Daphnia dentifera*, a freshwater zooplankton common in stratified lakes in the Midwestern United States (Tessier and Woodruff 2002, hereafter referred to as the host). While filter-feeding, hosts ingest infectious spores of the two parasites used in our study: the fungus *Metschnikowia bicuspidata* (hereafter referred to as 'fungi') and the bacterium *Pasteuria ramosa* (hereafter referred to as 'bacteria'). Both parasite species replicate within the host and only disperse into the environment upon host death (known as "obligate killers")(Ebert 2005). Fungal infection primarily reduces host lifespan, and bacterial infection primarily reduces host fecundity via castration in *D. dentifera* (Auld *et al.* 2012; Clay *et al.* 2019b). *D. dentifera* typically do not recover from either of these pathogens once they are fully infected (but see Stewart-Merrill & Cáceres 2018; Izhar *et al.* 2020; Stewart-Merrill *et al.* 2021 for exceptions). *Daphnia*-parasite interactions shift with age (e.g., Izhar et al. 2015, Clerc et al. 2015), likely due to a combination of factors including changes in immune function, physiology, energetics, and behavior of hosts.

In *Daphnia*-bacteria interactions, these shifts with age occur due to changes in host molting frequency and host gut structure (Izhar *et al.* 2020); changes in host gut structure with age should also impact interactions with the fungi (Stewart-Merrill & Cáceres 2018; Stewart-Merrill *et al.* 2021). We also expect strong changes in *Daphnia*-bacteria interactions as the host ages because the bacteria sterilize hosts, shunting resource allocation from reproduction to growth, and host energy allocation to reproduction shifts with age (Ebert 1996; Cressler *et al.* 2014; Clerc *et al.* 2015).

Experimental design

We used a clonal line of *D. dentifera* collected from Midland Lake in Indiana (strain "Mid37") that had been maintained asexually in lab conditions for several years at 20° C and a 16/8 light/dark cycle. To control for environmental effects, we kept individual hosts in 30 ml of filtered lake water in 50 ml beakers, and then used clonal offspring from the third clutch of those individuals in our experiments. Throughout the experiment, *D. dentifera* were individually kept in 15 ml centrifuge tubes filled with filtered lake water and fed 1 mg dry weight of live *Ankistrodesmus falcatus* (strain AJT: Schomaker & Dudycha 2021) algal food per ml per day. For infection assays in *D. dentifera*, we used the "Std" fungal isolate and the "G/18" bacterial isolate (Auld *et al.* 2014).

We exposed hosts to (i) no parasites, (ii) only bacteria, (iii) only fungi, (iv) bacteria first and then fungi three days later, or (v) fungi first and then bacteria three days later. To measure whether parasite interactions changed as hosts aged, we implemented each of these parasite exposure treatments on hosts of three different ages: 4, 12, or 20 days old (Table S1). Hosts were exposed to 1000 bacterial spores/ml or 200 fungal spores/ml, as bacterial spores are less

infectious than fungal spores, and thus require a higher dose to match fungal probability of infection; in addition, single infections with the bacteria yield many more spores at host death, as compared to the fungi (Clay et al. 2019b). Infectious spores were obtained by homogenizing Daphnia infected by only the bacteria or only the fungi. Thus, experimental animals were exposed to ground up *Daphnia* concurrently with infectious spores. To control for this exposure, whenever we exposed hosts to infectious spores, we pipetted homogenized, uninfected Daphnia into the tubes of all unexposed hosts, equal to the average number of Daphnia put in each parasite-exposed tubes on that infection date. After 24 hours of exposure, all hosts were placed in clean tubes with fresh water that did not contain spores. Each experimental treatment had 30 replicate Daphnia. Thus, across the entire experiment, we had 5 infection treatments x 3 age treatments x 30 replicates = 450 host individuals. Hosts were collected at death and stored frozen in 0.1 ml of milliQ water. Hosts were later ground up with a pellet pestle, and infectious fungal and bacterial spores were counted on a hemocytometer. Hosts were counted as "infected" by a parasite if we found mature infectious spores of that parasite inside the host. We measured whether parasites altered host feeding rate, and thus exposure to infectious spores of the other parasite (Fig. 1A), host susceptibility (Fig. 1B), and number of infectious spores released from each host (Fig. 1C).

By altering host feeding rate, parasites can alter the chance that the host would become infected by another parasite (Fig. 1A). Parasites can change host feeding rate in two ways: parasites can cause hosts to temporarily lower their feeding rate if hosts sense parasites in the environment (Strauss *et al.* 2019), or parasites can permanently change host feeding rate upon infection (Searle *et al.* 2016; Penczykowski *et al.* 2022). To test whether hosts lower their feeding rate in the presence of parasites and whether this changes with host age, we measured the

feeding rate of all hosts when they were exposed to parasites, and simultaneously measured the feeding rate of unexposed hosts of the same age. To test whether infection by a parasite had a long-term impact on feeding rate, we measured the feeding rate of infected hosts three days after parasite exposure, as well as the feeding rate of unexposed hosts of the same age (Table S1). To measure feeding rate, hosts were placed in 15 ml centrifuge tubes and fed 1 mg of A. falcatus per ml. These tubes, as well as control tubes with no hosts, were inverted every two hours for an 8hour feeding period. At the end of this period, we measured the fluorescence of samples taken from each tube. The difference in fluorescence between grazed and ungrazed tubes was used to calculate the feeding rate of the *Daphnia*. As both the fungi and bacteria are encountered passively in the water column, this also determines the number of infectious spores fed upon by the host. We further derived the feeding rate of hosts in ml/hour as in Sarnelle & Wilson (2008). Using the fitdist function in R (Delignette-Muller & Dutang 2015), we found that a gamma distribution fit to our model gave a lower AIC value than other probability distributions. Thus, we analyzed host feeding rate with the glm function in R using the gamma distribution and a log link function (version 4.0.4, 2021) where the parasite that hosts were exposed to during feeding trial (bacteria, fungi, no parasite), infection status (previously infected by bacteria, fungi, or no parasites), and host age (continuous variable) were used as explanatory variables to compare among feeding rates of uninfected, unexposed hosts and all other hosts.

We next calculated how prior infection and host age influenced host susceptibility to infectious spores (Fig. 1B). We assumed that each consumed spore had an independent probability of infecting the host. Thus, given that a host consumed U spores, and that the host has μ probability of becoming infected for each spore consumed, the likelihood of infection is given by the cumulative distribution function for an exponential function:

 $1 - e^{(-\mu U)} \qquad eq. 1$

We assumed that the per spore infection probability (μ) changes linearly with host age and is multiplied by a constant if the host was previously infected. We used the mle2 function in R to find (a) the μ intercept, (b) linear change in μ with host age, and (c) change in μ for prior infection that minimized the negative log-likelihood of producing our data, assuming a binomial distribution of infection probability.

Fluorometry readings for several days in the middle of our experiment had erroneous measurements (they estimated negative feeding rates for many samples), and so we only used feeding rate measurements for our oldest and youngest age groups. Thus, we did not test for polynomial terms in age-effects on feeding rate or host susceptibility. Additionally, we discarded any fluorometry readings that showed a negative feeding rate (9/404 readings from young and old hosts).

To measure how within-host interactions and host age at infection altered infectious spore release (Fig. 1C), we counted the number of infectious spores contained within the host at death; both parasites are obligate killers, with spores only released after host death. To calculate mean spore yield, we only included hosts that were successfully infected by all parasites to which they were exposed. We used the fitdist package in R to calculate the AIC values of various probability distributions fit to our spore release data. Bacterial spores best fit a gamma distribution, while fungal spores best fit a normal distribution. The number of bacterial spores released from infected hosts was analyzed with the glm function in R with a log link function, with age at bacterial infection, co-infection treatment (prior fungal infection, later fungal infection, no fungal infection), and interactions between age and co-infection treatment used as explanatory variables. The same analysis was conducted for the fungal parasite using the lm function in R.

For all outcomes that were used to parameterize our agent-based model (feeding rate, perspore susceptibility, spore yield, lifespan, and births/day), we ran a series of generalized linear models with increasing complexity ranging from intercept only to models where the outcome was a function of infection treatment, host age, host age squared (except where noted), and interactions between infection treatment and age variables. We report results from the model with the lowest AIC value.

Empirical Results and Translation to Agent Based Model

We examined how parasites interact within the host through three mechanistic pathways: host feeding rate, host susceptibility, and host spore yield (Fig. 1). In addition to measuring parasite interactions, we used the results of these experiments to parameterize an agent-based model of a multi-parasite epidemic in NetLogo (Wilensky 1999) to understand the implications of within-host interactions for epidemic dynamics. Thus, below we present the results of our experiments and show how they parameterized an agent-based model used to understand the implications of within-host interactions for the dynamics of epidemics.

In our agent-based model, populations reside in a volume, V, with a carrying capacity of K Daphnia/L. State variables B and F represent bacterial and fungal spores/ml. All hosts have variables for age (a), feeding rate (f), probability of infection per bacterial or fungal spore ingested $(\mu_B \text{ or } \mu_F)$, maximum offspring produced per day (b), number of bacterial or fungal spores released at death $(z_B \text{ or } z_F)$, and lifespan (l). Parameters for each host changed with age of host and day at which the host became infected, based on statistical analysis of empirical results. Model dynamics are in discrete time with timesteps of 1 day. Below we present model equations for host feeding rate, probability of infection, and spore yield for infected hosts. See supplement

for additional analysis and model equations for how infection altered host lifespan and reproduction (Supplemental Information: Host Fitness).

Host Feeding Rate

Feeding rate increased with host age, with parasites having non-significant effects. The only significant relationship in our model was that feeding rate increased with age (p < 0.001, Table S7, Figure S3). Infection and exposure to parasites all non-significantly decreased host feeding rate. Host age and infection treatment non-significantly interacted to decrease feeding rate when exposed to the fungi, and increase feeding rate when exposed to the bacteria (Table S7). Despite the large number of non-significant terms, this model was selected via AIC and so we incorporate all terms in our agent-based model (Table S6). Thus, the feeding rate (ml/day) of hosts in our agent-based model (f) is given by

$$f = e^{f_{int} + af_{slope} + I_i E_j f_{ij} + aI_i E_j f_{slope,ij}}$$
 eq. 2

where f_{int} indicates the feeding rate intercept, a is host age, f_{slope} is the change in feeding rate with host age, I_i indicates whether the host has been infected by either or no parasite, E_j indicates whether the host is currently exposed to either or no parasite, and $f_{slope,ij}$ indicates the additional change in feeding rate with host age for host infected by i and exposed to j. Since we analyzed data with a gamma distribution and a log-link, we take the exponent of parameters to match model output.

Host susceptibility

Prior infection in young hosts altered the per-spore probability of infection for both the bacteria and the fungi, though this effect disappeared in older hosts (Fig. 2, Tables S8-S11). For

uninfected hosts exposed to bacteria, per spore infection probability decreased from age 4 to age 20 days by approximately 78% (p < 0.001; black line in Fig. 2A), consistent with prior studies (Izhar & Ben-Ami 2015). Prior fungal infection decreased bacterial infection probability in young hosts but did not affect infection in older hosts (Fig. 2A). In our statistical model, this translates to prior fungal infection decreasing bacterial infection probability (p<0.001), and prior fungal infection interacting with host age to lessen the negative impact of age on bacterial infection probability (p<0.001). For uninfected hosts exposed to fungi, per spore infection probability increased from age 4 to age 20 days by approximately 20% (p < 0.001; black line in Fig. 2B). Prior bacterial infection increased fungal infection probability in young hosts but did not affect infection in older hosts (Fig. 2B). In our statistical model, this translates to prior bacterial infection increasing fungal infection probability (p<0.001), and prior bacterial infection interacting with host age to create a negative impact of age on fungal infection probability (p<0.001).

In our model, the number of spores that hosts consume each day is given by the volume of water filtered by hosts each day (f) multiplied by the density of spores in the environment (B or F). Based on our empirical results, the probability of becoming infected after consuming a single spore of parasite i is given by

$$\mu_i = \mu_{i,int} + \mu_{j.prior}I_j + a(\mu_{i,a} + \mu_{j.prior,a}I_j)$$
 eq. 3

where $\mu_{i,int}$ is the infectivity intercept for parasite i, $\mu_{j,prior}$ is the change in infectivity if hosts were previously infected by the other parasite, $\mu_{i,a}$ is change in infectivity due to age, a, $\mu_{j,prior,a}$ is the additional change in host infectivity due to age for hosts previously infected by the other parasite, and I_j is an indicator variable that is 1 if the host was previously infected by

the other parasite and 0 if not. (See tables S6 and S7 for parameter values and all p-values.) The probability of becoming infected by parasite i for each timestep is given in eq. 1. We found no evidence that secondary infection by either parasite reduced the infection prevalence of the first arriving parasite, which would signal superinfection (p=0.89 for fungal superinfection, p=0.85 for bacterial superinfection).

Spore Yield

Co-infection and host age squared jointly altered bacterial spore yield, but not fungal spore yield (Fig. 3A, Tables S12, S13). In single infections, bacterial spore yield of hosts exposed at 20 days old was 43% that of hosts exposed at 4 days old (p=0.0265). If the bacteria arrived first in co-infected hosts, co-infection reduced bacterial spore yield at the intercept by 76% (p<0.001; compare blue and green symbols and lines, Fig. 3A) and spore yield doubled as age at infection increased from 4 to 20 days (p=0.0116; green symbols and line, Fig. 3A). If the fungi arrived first in co-infected hosts, co-infection did not change bacterial spore yield at the intercept (p=0.7832), but the decrease in spores with age at infection was greater, reducing spore yield by almost 100% for hosts infected at day 20 (p<0.001; compare blue and yellow symbols and lines, Fig. 3A). There were no significant differences between treatments in the number of fungal spores released by infected hosts (Fig. 3B, Tables S14 and S15).

As AIC model selection indicated that bacterial spore yield is a function of infection status and host age at bacterial infection squared, as well as interactions between infection status and age at bacterial infection squared, the number of bacterial spores that infected hosts will release upon death in our agent-based model is

$$\beta_B = e^{\beta_{B,int} + \beta_{B1}I_{B1} + \beta_{B2}I_{B2} + \gamma_B^2(\beta_{B,a} + \beta_{B1,a}I_{B1} + \beta_{B2,a}I_{B2})} eq. 4$$

where $\beta_{B,int}$ is the intercept of bacterial spores released, β_{B1} is the constant change in spore yield in co-infected hosts where the bacteria arrived first, γ_B is the age at which the bacteria infected the host, $\beta_{B,a}$ is the change in spore yield with age at infection, $\beta_{B1,a}$ is the additional change in spore yield with age at infection in co-infected hosts where the bacteria arrives first, $\beta_{B12,a}$ is the additional change in spore yield with age at infection in co-infected hosts where the bacteria arrives second, I_{B1} is an indicator variable that is 1 if the host was infected by the fungi after bacterial exposure and 0 if not, and I_{B2} is an indicator variable that is 1 if the host was infected by the bacteria after the fungi and 0 if not. (See Table S8 for all parameter values.) Model coefficients are reported in terms of log spores, so spore yield is an exponential function of the model coefficients.

Since fungal spore yield from infected hosts did not change with age or infection treatment (Tables S14, S15), the amount of fungal spores that a host releases upon death (β_F) if they are infected is equal to an exponential function of a constant intercept, $\beta_{F,int}$:

$$\beta_F = e^{\beta_{F,int}} eq.5$$

To see the combined effect of host feeding rate, susceptibility, and parasite spore yield on parasite success (i.e., the probability that an exposed host would become infected multiplied by the average number of infectious spores released from a host) in singly infected and co-infected hosts, see the section entitled "Total Parasite Fitness" in the supplement (Fig. S4-5, Table S17).

Running the agent-based model

We simulated epidemics in our agent-based model and compared dynamics of fungal and bacterial epidemics when they occurred alone vs. when they co-occurred. We also simulated

population dynamics with no parasites. To initialize our model, we generated KV agents (i.e., set the population at carrying capacity), each with an age drawn from a normal distribution with a mean of either 8, 14, or 20 days and a standard deviation of 10 days. (Hosts could not have a negative age). Increasing standard deviation decreases amplitude of host population cycles, but otherwise does not alter model outcomes. We then randomly assigned 5% of agents to be infected with the fungi if the run was in the "fungi alone" or "co-infected" treatment, and randomly assigned 5% of agents to be infected with the bacteria if the run was in the "bacteria alone" or "co-infected" treatment. These infected agents were assigned an "age at infection" $(\gamma_B \text{ or } \gamma_F)$ randomly drawn between 1 and their age. At each timestep of our model, we first increased the age of all agents by 1 day. If the age of the agent is greater than the lifespan of the agent based on eq. S1, then the agent dies, and adds a number (given by eq. 4 and 5) of infectious spores of one or both pathogens to the water, depending on the agent's infection status. For both parasites, there is minimum number of days that must pass between when hosts become infected and when the host produces mature infectious spores. Thus, if a host died less than ten days after being infected by a parasite, the agent does not release spores of that parasite. Because, as described above, infected individuals were at a range of days post-infection, some of the individuals at the start of the experiment were already 10 (or more) days post-infection and therefore could release spores at death even during the first timestep.

Agents become infected by encountering spores while filtering water; the number of spores that an agent consumes is given by the volume of water filtered by hosts each day (f, given in eq. 2) multiplied by the density of spores in the environment (B or F). The probability that an agent will be infected with a given pathogen is then determined by the per-spore probability of infection (eq. 3), which is then entered into eq. 1. If agents are infected, they are

assigned an "age at infection" (γ_B or γ_F) equal to their age. Any spore an agent consumes is removed from the water column, and each spore has a probability of degrading at each time step. Finally, at each timestep, each host has a probability of creating one uninfected agent, with a probability of b(1 - K/N), where b is the offspring per day calculated in eq. S2.

To mirror epidemics in the field, we ran our model forward for 120 days, slightly longer than the time over which we annually observe epidemics. We draw the ages of hosts at the beginning of our epidemic from a normal distribution with mean = 14 and standard deviation = 10 days, setting any draws < 1 equal to 1 day (we additionally tested impact of setting initial age to 8 or 20 days, Fig. 4). We tested variation in initial conditions of age structure and find that they largely do not have an impact on epidemic dynamics due to the stabilizing effects of host evolution (host evolution described below, stabilizing effect described below, shown in Fig. 4). In our system, hosts evolve resistance to infection (Duffy & Sivars-Becker 2007) and parasite transmission decreases over the epidemic season (Duffy et al. 2009). Following Duffy et al. (2009), we assume that epidemics end due to hosts evolving decreased susceptibility to infection, which in the terms of our model means decreased per-spore infection probability. When generating individual hosts at the first timestep of our model, we draw values of $\mu_{B,int}$ and $\mu_{F,int}$ (eq. 3) for each host from gamma distributions with global mean values taken from experimental results (Tables S9, Table S11), and variance values v_B and v_F . Following Duffy et al. (2009), at each timestep we reduce the global values of $\mu_{i,int}$ by $v_i \frac{I_i}{N}$, where $\frac{I_i}{N}$ is the prevalence of parasite i. Any hosts born during that timestep then have their individual values of $\mu_{i,int}$ drawn from a gamma distribution with the updated global value of $\mu_{i,int}$. Thus, host susceptibility to infection decreases over time as a function of infection prevalence. We set values of v_B and v_F such that bacterial epidemics in the absence of the fungi peaked at ~30%

prevalence and fungal epidemics in the absence of the bacteria peaked at ~20%, mirroring field patterns in our system. At each 1-day timestep, we recorded the number of uninfected, bacteria infected, fungi infected, or co-infected agents, their average age, and the average age of individuals infected at each time step.

We report population-scale model results in terms of fungal and bacterial infection prevalence. We find that the results are unchanged if we report the density of hosts infected by the fungi and the bacteria instead (Figure S6,7).

Modelling Results

Variation in initial age structure and stabilizing effect of host evolution

To understand the impact of variation in host age structure on epidemic dynamics, we varied the mean age of hosts at the beginning of simulations, and the age at infection for individuals seeding epidemics (Fig. 4). In these simulations, epidemiologically relevant parameters (feeding rate, per-spore susceptibility, spore yield, and births per day) varied with host age. We find that initial age structure had a slight impact on epidemic shape. As we increased the age of hosts at the beginning of the epidemic, we decreased time until death for infected individuals, and therefore time until parasite transmission. Thus, when hosts were older at the beginning of simulations, we see more rapid increases in infection prevalence compared to simulations when hosts were initially younger.

However, we see that these initial rapid increases in infection prevalence do not translate to larger overall epidemic sizes in simulations with older initial host populations (as indicated by the relatively consistent heights of the vertical bars in Fig. 4). This is because high initial

infection prevalence leads to faster evolution of decreased host susceptibility, slowing transmission. Thus, the impact of initial age structure on epidemic size is weakened due to host evolution – epidemics must reach a certain size to drive host susceptibility low enough for the epidemic to end, and thus epidemics all have similar peaks and durations.

Impact of age effects on epidemic dynamics

We next examined how age structure alters the impact of coinfection at the hostpopulation scale. In running this analysis, we compared results from our full population scale model (where epidemiologically relevant parameters varied with age, as measured above) to a population scale model where we parameterized our model with data from a single age. Individuals in our single-age parameterization still had a variety of ages. However, they all had the same probability of becoming infected, based on experimental results from hosts of a single age (4, 12, or 20 days). Once infected, we also set the "age at infection" parameter (γ_i) equal to that age when calculating spore yield and host feeding rate. Thus, in our three "fixed parameter" models, individuals varied in age, but feeding rate, per-spore susceptibility, spore yield, and births per day were constant – that is, those epidemiologically relevant parameters did not vary with host age. The comparison between our full model (with parameters that vary with age, as measured empirically) and our three set-age models (where parameters did not vary with age) is useful for two reasons. First, by removing the link between age structure and transmission parameters, we can isolate the impact of age-induced variability and age-mediated feedback loops (Fig. 1) on epidemic dynamics. Second, infection assays used to parameterize host population-scale coinfection models are generally conducted on hosts that are a single age. Thus, each set-age scenario represents conclusions that researchers would come to regarding the impact of coinfection at the host-population level if they did not take age-effects into account. We use

prevalence as a response variable when analyzing our simulation results, though our results do not qualitatively differ when using density of infected hosts as a response metric (Fig. S6,S7). Higher peaks indicate higher parasite transmission, which drives a more rapid evolution of low host susceptibility.

When the epidemiologically relevant parameters are held constant within a population, increasing host age can increase or decrease peak fungal infection prevalence, depending on the presence of co-infections. In the absence of the bacteria, increasing the age at infection increases peak fungal infection prevalence (from 0.14 when age = 4 to 0.24 when age = 20, Fig. 5, top row, first three panels, red lines) because older hosts have a higher susceptibility to fungal infection (Fig. 2B). In the presence of the bacteria however, increasing the age at infection modestly decreases peak fungal infection prevalence (from 0.47 when age = 4 to 0.39 when age = 20, Fig. 5, top row, first three panels, purple lines) because prior bacterial infection increases host susceptibility to fungal infections in young hosts, but not in older hosts (Fig. 2B). Because the facilitative effect of the bacteria only exists in younger hosts, the facilitative effect of bacteria on fungi at the host population scale decreases as the age at infection becomes higher (Fig. 5, top row, first three panels, difference between red and purple lines).

When epidemiologically relevant parameters are held constant within a population, ageeffects have consistent impacts on peak bacterial prevalence in singly- and co-infected
populations: peak bacterial prevalence decreases with increasing age at infection in both singlyand co-infected populations (from 0.50 when age = 4 to 0.35 when age = 20 in the absence of the
fungi, and from 0.38 when age = 4 to 0.28 when age = 20 in the presence of the fungi, Fig. 5,
bottom row, first three panels). Increasing age at infection decreases peak bacterial infection
prevalence because younger hosts have a higher susceptibility to bacterial infection regardless of

prior infection status (Fig. 2A), and because bacterial spore yield generally decreases with age (Fig. 3A). Because prior fungal infection decreases host susceptibility to the bacteria the most in young hosts, co-infection decreases peak bacterial prevalence the most when age at infection is 4 days (Fig. 5, bottom row, largest difference between purple and blue lines in the first panel).

We now ask how intraspecific variation in parasite interactions due to age-effects alters disease dynamics. To do this we compare previous simulations (where epidemiologically relevant parameters did not vary with age, and were set based on estimates of hosts at a single age) to simulations where we allowed epidemiologically relevant parameters (per spore susceptibility, feeding rate, spore yield, and birth rate) to vary with age, as measured empirically. We find that incorporating the variation in these parameters with age mostly eliminates the impact of co-infection on infection prevalence (Fig. 5, "Age Varies" panels), as the 95% envelopes of infection prevalence from stochastic runs in singly infected and coinfected scenarios now heavily overlap. This mostly happens because age variation lowers bacterial infection prevalence in singly infected populations and lowers fungal infection prevalence in co-infected populations.

Allowing epidemiologically relevant parameters to vary with age lowers the prevalence of the bacteria in singly infected populations because of the way feeding rate and the probability of bacterial infection change with host age in the absence of the fungi. As hosts age, their feeding rate increases, increasing the number of spores they consume, but hosts are less susceptible to being infected by each spore (Fig. 2,S3). This results in a non-linear relationship between host age and probability of infection for a given density of spores in the environment (Fig. 6C). The probability of infection is relatively steady through age 21 days, before dropping steeply to 0. Thus, when we derive infection parameters in our model from hosts aged 4, 12, or 20 days,

infection probabilities do not change much between scenarios. However, allowing epidemiologically relevant parameters in our model to reflect the actual age distribution gives us older individuals who are immune to infection, thus lowering overall prevalence. In coinfected populations, older individuals have a higher probability of being infected by the bacteria (Fig. 6), but a lower spore yield overall (Fig. 3) leading to a negligible impact of coinfection on bacterial prevalence.

Allowing epidemiologically relevant parameters to vary with age eliminates the positive impact of coinfection on fungal prevalence for similar reasons as it eliminates the impact of coinfection on bacterial prevalence. Prior infection with the bacteria boosts the likelihood that hosts below 21 days old would be infected by the fungi and eliminates the probability that hosts above the age of 23 days would be infected by the fungi (Fig. 6 A,B). Thus, when parameterizing parasite interactions with only hosts of age 4, 12, or 20 days, we see only the positive effects of coinfection. However, taking the full age structure into account, increases in fungal prevalence due to increased infection probability in younger hosts are balanced by decreases in fungal prevalence due to decreased infection probability in older hosts. Ultimately, these results indicate that the full age structure of a population must be considered to understand how parasite interactions at the host scale will translate to the host-population scale.

Discussion

Host age alters how parasites interact within their hosts, but we lacked an understanding of how these age effects alter multi-parasite epidemics. Our study shows that, in a co-infected zooplankton system, within-host interactions altered host susceptibility and spore yield at the single host scale (Figure 2,3). However, age variation among a host population, along with the

way epidemiologically relevant parameters change with host age, can eliminate the impact of coinfection on epidemic dynamics (Fig. 5). For the bacteria, our models indicate that coinfection
lowers spore yield and infection probabilities in younger hosts, but at the population scale this
negative impact of coinfection is counterbalanced by coinfection increasing infection
probabilities in older hosts (Fig. 3,6). For the fungi, our model indicates that coinfection
increases infection probabilities in younger hosts, but at the population scale this positive impact
of coinfection is counterbalanced by coinfection lowering infection probabilities in older hosts.
Thus, we demonstrate that population-level impacts of coinfection in this system cannot be
approximated when parameterizing the model with hosts infected at a single age, as coinfection
models generally do.

Without considering how traits such as per spore susceptibility, feeding rate, and spore yield change with age, we may incorrectly estimate the impact of co-infection on epidemic dynamics. Experimental measurements of within-host interactions can be scaled up to predict multi-parasite epidemic dynamics (Marchetto & Power 2017; Rynkiewicz *et al.* 2017). However, experiments on within-host interactions are often conducted on hosts of a single, relatively young age (Ben-Ami 2019). This method prevents models from including age-mediated feedback loops, where parasite transmission determines the age of infection, which determines how parasites interact within a host, which loops back to determine parasite transmission. In our system, models parameterized with experiments performed on a single host age overestimate the impact of co-infection on infection prevalence over the course of an epidemic (Fig. 5); this effect is particularly strong for the scenario that uses the youngest hosts. We may see similar results in other systems. Some past research has measured within-host interactions in wild hosts, and, as such, measured interactions across a wide range of host ages (Fenton *et al.* 2010; Halliday *et al.*

2018). This approach could potentially quantify the impact of age on within-host interactions. However, if this approach is used to predict an average strength of within-host interactions for all hosts, this again removes the possibility of quantifying age-mediated feedback loops that can drive multi-parasite dynamics. One way to ease data collection on how age-effects alter parasite interactions is to quantify age-size relationships, as age and size are highly correlated in many taxa and size is easier to measure than age. However, especially when attempting to quantify age-effects in the wild using body size, it is also important to consider other potential confounding factors, such as resource variation between populations, the impact of infection on host size (Cressler *et al.* 2014), as well as other factors that complicate inferring parasite interactions from natural populations (Telfer *et al.* 2008).

If host age alters within-host interactions, then the impact of co-infection on epidemic dynamics depends on the age structure in host populations. Many organisms reproduce seasonally (e.g., Carter et al. 2018), meaning that the mean age of hosts in a population changes over time. In these species, the strength of within-host interactions may systematically change throughout the year. For instance, in our system, within-host interactions can have opposite effects in young vs. old hosts (Fig. 6). Thus, for a seasonally breading species, the impact of co-infection on epidemic dynamics may change with time after the breeding season, as the host population ages. Further, epidemics themselves can change the age structure of a population (Dwyer 1991; Hite *et al.* 2016). Thus, we can expect the strength of within-host interactions to change over the course of an epidemic in response to parasite-driven shifts in mean host age. Quantifying how multi-parasite epidemics change host age structure, and how host age structure in turn alters multi-parasite dynamics, will further our understanding of age-mediated feedback loops in co-infected systems.

Epidemics in wild *Daphmia* populations exhibit high spatial and temporal variation (Duncan & Little 2007; Duffy *et al.* 2010; Goren & Ben-Ami 2013; Shaw *et al.* 2020). In addition to abiotic factors (Shaw *et al.* 2020), predation (Auld *et al.* 2014b), and variation in the species composition of the host community (Strauss *et al.* 2016), we have suggested that coinfection may play a role in driving variation in epidemic size (Clay *et al.* 2019b, 2020). Our results indicate that once variation in host age is considered, this is likely not the case, at least for this pair of parasites. However, before we can remove co-infection from our list of possible causes for variation in epidemic size, we must reconcile the results of this study with evidence from lab populations of *Daphmia* where the presence of the fungal pathogen significantly reduces the prevalence of the bacterial pathogen (Clay *et al.* 2020). One possible explanation is that infection prevalence of parasites can be much higher in lab populations than observed in natural populations of *Daphmia*, and higher infection prevalence likely leads to stronger parasite interactions at the population scale.

Our experimental results show that the impact of co-infection on parasite fitness weakens as hosts age (though for spore yield this depends on the order of infection), a pattern that we may find across systems. Our bacterial parasite exhibits strong genotype by genotype effects with *Daphnia* hosts (Ben-Ami & Routtu 2013), and *Daphnia* genotypes differ substantially in key traits associated with their interactions with our fungal parasite (Duffy *et al.* 2012; Searle *et al.* 2016; Paraskevopoulou *et al.* 2022; Penczykowski *et al.* 2022). Thus, some of our empirical results may vary depending on the genotypes in a particular population. However, certain aspects of our empirical results will likely generalize. We hypothesize that the main impact of fungal infection on bacterial spore yield in our system is that fungal infection reduces host lifespan, reducing the time that bacterial spores have to replicate before host death (Auld *et al.* 2014).

Thus, fungal impact on bacterial spore yield is minimized by infecting old hosts where there is little difference between time to death due to senescence and time to death due to fungal infection (Fig. 5); we encourage future studies comparing host species that differ in overall lifespan (e.g., relatively short-lived *Ceriodaphnia* vs. relatively long-lived *D. magna*) to see if age-effects on co-infection are consistent as well as take advantage of the high frequency of co-infection in some *Daphnia* populations (e.g., Goren and Ben-Ami 2013) to test these relationships in natural communities. We also encourage future studies of hosts with co-infecting parasite species that differ in their transmission mode, host exploitation strategy, priority effects and overall virulence. Further, we may see the impact of co-infection on parasite fitness weaken in older hosts in other systems where parasites largely impact one another by reducing the duration of infection, either by reducing host lifespan (Ezenwa & Jolles 2015) or via superinfection (Curtis & Tanner 1999; Ben-Ami 2019).

Ultimately, to improve our understanding of how age-effects alter multi-parasite systems, we must move away from understanding co-infection dynamics phenomenologically, and toward understanding them mechanistically. Within-host interactions depend on many factors such as resource availability (Wale *et al.* 2017), order of infection (Ben-Ami & Routtu 2013; Clay *et al.* 2019a; Karvonen *et al.* 2019), and timing between infections (Adame-Álvarez *et al.* 2014), as well as host age (Izhar & Ben-Ami 2015; Izhar *et al.* 2015). To truly understand how within-host interactions scale up to alter multi-parasite epidemics we need to understand how each of these factors interact with one another simultaneously. Rather than accomplishing this via impractically large factorial experiments, we need to build a mechanistic understanding of within-host interactions that will allow accurate predictions of within-host interactions under various circumstances. One potential is to analyze host age-effects and co-infection using

dynamic energy budget models (Hall *et al.* 2009; Cressler *et al.* 2014). This approach will be particularly useful given that many within-host parasite interactions are resource mediated (Graham 2008). Our study has shown that taking age effects into account can alter qualitative predictions about the impact of co-infection (e.g., in our study we move from predicting that co-infection will decrease or increase epidemic size to predicting that co-infection will have no impact on epidemic dynamics given the contradicting age-dependent effects of fungal vs. bacterial infections). We suggest that mechanistic models of parasite interactions are the most efficient way to incorporate age effects into co-infection models across systems.

Acknowledgments

We thank Rebecca Bilich for assistance in the lab. This work was supported by NSF DEB-1748729 to MAD and grant #938/16 from the Israel Science Foundation (ISF) to FBA. MAD also acknowledges support from the Moore Foundation (GBMF9202; DOI: https://doi.org/10.37807/GBMF9202).

Statement of authorship

PAC and MAD conceptualized and planned experiments with input from SG and FB. PAC, JG, VH, and SG ran experiments. PAC conducted statistical analysis and modelling. PAC primarily wrote manuscript with feedback and editing by all authors.

Data and Code Accessibility

All data and code can be accessed at Dryad repository (Clay 2023, https://datadryad.org/stash/dataset/doi:10.5061/dryad.jh9w0vtbv).

Literature Cited

- Abu-Raddad, L.J., Magaret, A.S., Celum, C., Wald, A., Longini, I.M., Self, S.G., *et al.* (2008). Genital herpes has played a more important role than any other sexually transmitted infection in driving HIV prevalence in Africa. *PLoS One*, 3, e2230.
- Abu-Raddad, L.J., Patnaik, P. & Kublin, J.G. (2006). Dual infection with HIV and malaria fuels the spread of both diseases in sub-Saharan Africa. *Science*, 314, 1603–6.
- Adame-Álvarez, R.-M., Mendiola-Soto, J. & Heil, M. (2014). Order of arrival shifts endophyte-pathogen interactions in bean from resistance induction to disease facilitation. *FEMS Microbiol. Lett.*, 355, 100–107.
- Anderson, R.M. & May, R.M. (1985). Age-related changes in the rate of disease transmission: Implications for the design of vaccination programmes. *J. Hyg. (Lond).*, 94, 365–436.
- Auld, S.K.J.R., Hall, S.R., Duffy, M.A., Tessier, A. & Cáceres, C. (2012). Epidemiology of a daphnia-multiparasite system and its implications for the red queen. *PLoS One*, 7, e39564.
- Auld, S.K.J.R., Hall, S.R., Housley Ochs, J., Sebastian, M. & Duffy, M.A. (2014a). Predators and patterns of within-host growth can mediate both among-host competition and evolution of transmission potential of parasites. Am. Nat., S77-90.
- Auld, S.K.J.R., Hall, S.R., Housley Ochs, J., Sebastian, M. & Duffy, M.A. (2014b). Predators and patterns of within-host growth can mediate both among-host competition and evolution of transmission potential of parasites. *Am. Nat.*, 184 Suppl 1, S77-90.
- Ben-Ami, F. (2019). Host age effects in invertebrates: epidemiological, ecological, and evolutionary Implications. *Trends Parasitol.*, 35, 466–480.
- Ben-Ami, F., Rigaud, T. & Ebert, D. (2011). The expression of virulence during double infections by different parasites with conflicting host exploitation and transmission strategies. J. Evol. Biol., 24, 1307–1316.
- Ben-Ami, F. & Routtu, J. (2013). The expression and evolution of virulence in multiple infections: the role of specificity, relative virulence and relative dose. *BMC Evol. Biol.*, 13, 97.

- Carter, S.K., Saenz, D. & Rudolf, V.H.W. (2018). Shifts in phenological distributions reshape interaction potential in natural communities. *Ecol. Lett.*, 21, 1143–1151.
- Clark, J., McNally, L. & Little, T.J. (2021). Pathogen dynamics across the diversity of aging. Am. Nat., 197, 203–215.
- Clay, P. A. 2023. Data for: Age structure eliminates the impact of coinfection on epidemic dynamics in a freshwater zooplankton system. American Naturalist, Dryad, Dataset, https://doi.org/10.5061/dryad.jh9w0vtbv
- Clay, P.A., Cortez, M.H., Duffy, M.A. & Rudolf, V.H.W. (2019a). Priority effects within coinfected hosts can drive unexpected population-scale patterns of parasite prevalence. *Oikos*, 128, 571–583.
- Clay, P.A., Dhir, K., Rudolf, V.H.W. & Duffy, M.A. (2019b). Within-host priority effects systematically alter pathogen coexistence. *Am. Nat.*, 193, 187–199.
- Clay, P.A., Duffy, M.A. & Rudolf, V.H.W. (2020). Within-host priority effects and epidemic timing determine outbreak severity in co-infected populations. Proceedings of the Royal Society B 287, 20200046.
- Clerc, M., Ebert, D. & Hall, M.D. (2015). Expression of parasite genetic variation changes over the course of infection: implications of within-host dynamics for the evolution of virulence. Proceedings of the Royal Society B 282.
- Cressler, C.E., Nelson, W.A., Day, T. & McCauley, E. (2014). Starvation reveals the cause of infection-induced castration and gigantism. Proceedings of the Royal Society B 281, 20141087.
- Curtis, L.A. & Tanner, N.L. (1999). Trematode accumulation by the estuarine gastropod Ilyanassa obsoleta. J. Parasitol., 85, 419.
- Delignette-Muller, M.L. & Dutang, C. (2015). fitdistrplus: An R package for fitting distributions. *J. Stat. Softw.*, 64, 1–34.
- Demott, W.R., Mckinney, E.N. & Tessier, A.J. (2010). Ontogeny of digestion in Daphnia: implications for the effectiveness of algal defenses. *Ecology*, 91, 540–548.

- Duffy, M.A., Cáceres, C.E., Hall, S.R., Tessier, A.J. & Ives, A.R. (2010). Temporal, spatial, and between-host comparisons of patterns of parasitism in lake zooplankton. *Ecology*, 91, 3322–3331.
- Duffy, M.A., Hall, S.R., Càceres, C.E. & Ives, A.R. (2009). Rapid evolution, seasonality, and the termination of parasite epidemics. *Ecology*, 90, 1441–1448.
- Duffy, M.A., Ochs, J.H., Penczykowski, R.M., Civitello, D.J., Klausmeier, C.A. & Hall, S.R. (2012). Ecological context influences epidemic size and parasite-driven evolution. *Science* (80-.)., 335, 1636–1638.
- Duffy, M.A. & Sivars-Becker, L. (2007). Rapid evolution and ecological host-parasite dynamics. *Ecol. Lett.*, 10, 44–53.
- Duncan, A.B., Agnew, P., Noel, V. & Michalakis, Y. (2015). The consequences of co-infections for parasite transmission in the mosquito *Aedes aegypti. J. Anim. Ecol.*, 84, 498–508.
- Duncan, A.B. & Little, T.J. (2007). Parasite-driven genetic change in a natural population of Daphnia. *Evolution (N. Y).*, 61, 796–803.
- Dwyer, G. (1991). The roles of density, stage, and patchiness in the transmission of an insect virus. *Ecology*, 72, 559–574.
- Ebert, D. (1996). Development, life cycle, ultrastructure and phylogenetic position of Pasteuria ramosa Metchnikoff 1888: Rediscovery of an obligate endoparasite of Daphnia magna Straus. *Philos. Trans. R. Soc. B Biol. Sci.*, 351, 1689–1701.
- Ebert, D. & National Center for Biotechnology Information (U.S.). (2005). Ecology, epidemiology, and evolution of parasitism in Daphnia.
- Ezenwa, V.O., Etienne, R.S., Luikart, G., Beja-Pereira, A. & Jolles, A.E. (2010). Hidden consequences of living in a wormy world: nematode- induced immune suppression facilitates tuberculosis invasion in African buffalo. *Am. Nat.*, 176, 613–24.
- Ezenwa, V.O. & Jolles, A.E. (2015). Opposite effects of anthelmintic treatment on microbial infection at individual versus population scales. *Science* (80-.)., 347, 175–177.

- Fenton, A., Lamb, T. & Graham, A.L. (2008). Optimality analysis of Th1/Th2 immune responses during microparasite-macroparasite co-infection, with epidemiological feedbacks.

 Parasitology, 135, 841–853.
- Fenton, A., Viney, M.E. & Lello, J. (2010). Detecting interspecific macroparasite interactions from ecological data: patterns and process. *Ecol. Lett.*, 13, 606–615.
- Finkenstädt, B.F. & Grenfell, B.T. (2000). Time series modelling of childhood diseases: a dynamical systems approach. *J. R. Stat. Soc. Ser. C (Applied Stat.*, 49, 187–205.
- Forseth, T., Ugedal, O. & Jonsson, B. (1994). The energy budget, niche shift, reproduction and growth in a population of arctic charr, Salvelinus alpinus. *J. Anim. Ecol.*, 63, 116.
- Goren, L. & Ben-Ami, F. (2013). Ecological correlates between cladocerans and their endoparasites from permanent and rain pools: Patterns in community composition and diversity. *Hydrobiologia*, 701, 13–23.
- Goren, L. & Ben-Ami, F. (2017). To eat or not to eat infected food: a bug's dilemma. *Hydrobiologia*, 798, 25–32.
- Graham, A.L. (2008). Ecological rules governing helminth-microparasite coinfection.

 Proceedings of the National Academy of Sciences of the U. S. A., 105, 566–70.
- Hall, S.R., Simonis, J.L., Nisbet, R.M., Tessier, A.J. & Cáceres, C.E. (2009). Resource ecology of virulence in a planktonic host-parasite system: an explanation using dynamic energy budgets. Am. Nat., 174, 149–162.
- Halliday, F.W., Penczykowski, R.M., Barrès, B., Eck, J.L., Numminen, E. & Laine, A.-L. (2020). Facilitative priority effects drive parasite assembly under coinfection. *bioRxiv*, 2020.03.30.015495.
- Halliday, F.W., Umbanhowar, J. & Mitchell, C.E. (2018). A host immune hormone modifies parasite species interactions and epidemics: insights from a field manipulation. Proceedings of the Royal Society B 285, 20182075.
- Hamilton, W.D. (1966). The moulding of senescence by natural selection. *J. Theor. Biol.*, 12, 12–45.

- Hite, J.L., Penczykowski, R.M., Shocket, M.S., Strauss, A.T., Orlando, P.A., Duffy, M.A., et al.
 - (2016). Parasites destabilize host populations by shifting stage-structured interactions. *Ecology*, 97, 439–449.
- Izhar, R. & Ben-Ami, F. (2015). Host age modulates parasite infectivity, virulence and reproduction. J. Anim. Ecol., 84, 1018–1028.
- Izhar, R., Gilboa, C. & Ben- Ami, F. (2020). Disentangling the steps of the infection process responsible for juvenile disease susceptibility. *Funct. Ecol.*, 1365-2435.13580.
- Izhar, R., Routtu, J. & Ben-Ami, F. (2015). Host age modulates within-host parasite competition. Biol. Lett., 11, 20150131.
- Karban, R. & English-Loeb, G. (1997). Tachinid parasitoids affect host plant choice by caterpillars to increase caterpillar survival. *Ecology*, 78, 603–611.
- Karvonen, A., Jokela, J. & Laine, A.-L. (2019). Importance of sequence and timing in parasite coinfections. *Trends Parasitol.*, 35, 109–118.
- Marchetto, K.M. & Power, A.G. (2017). Coinfection timing drives host population dynamics through changes in virulence. *Am. Nat.*, 91, 173–183.
- Paraskevopoulou, S., Gattis, S. & Ben-Ami, F. (2022). Parasite resistance and parasite tolerance: Insights into transgenerational immune priming in an invertebrate host. *Biol. Lett.*, In Press.
- Penczykowski, R.M., Shocket, M.S., Ochs, J.H., Lemanski, B.C.P., Sundar, H., Duffy, M.A., et al. (2022). Virulent disease epidemics can increase host density by depressing foraging of hosts. Am. Nat., 199, 75–90.
- Poulin, R. (1993). Age-dependent effects of parasites on anti-predator responses in two New Zealand freshwater fish. *Oecologia*, 96, 431–438.
- Raberg, L., de Roode, J.C., Bell, A.S., Stamou, P., Gray, D. & Read, A.F. (2006). The role of immune-mediated apparent competition in genetically diverse malaria infections. *Am. Nat.*, 168, 41–53.
- Rohani, P., Green, C.J., Mantilla-Beniers, N.B. & Grenfell, B.T. (2003). Ecological interference between fatal diseases. *Nature*, 422, 885–8.

- Rynkiewicz, E.C., Brown, J., Tufts, D.M., Huang, C.-I., Kampen, H., Bent, S.J., et al. (2017).
 Closely-related Borrelia burgdorferi (sensu stricto) strains exhibit similar fitness in single infections and asymmetric competition in multiple infections. *Parasit. Vectors*, 10, 64.
- Sarnelle, O. & Wilson, A.E. (2008). Type III functional response in daphnia. *Ecology*, 89, 1723–1732.
- Schomaker, R.A. & Dudycha, J.L. (2021). De novo transcriptome assembly of the green alga Ankistrodesmus falcatus. *PLoS One*, 16, e0251668.
- Searle, C.L., Cortez, M.H., Hunsberger, K.K., Grippi, D.C., Oleksy, I.A., Shaw, C.L., et al. (2016). Population density, not host competence, drives patterns of disease in an invaded community. Am. Nat., 188, 554–566.
- Shaw, C.L., Hall, S.R., Overholt, E.P., Cáceres, C.E., Williamson, C.E. & Duffy, M.A. (2020). Shedding light on environmentally transmitted parasites: lighter conditions within lakes restrict epidemic size. *Ecology*, 101, e03168.
- Simon, A.K., Hollander, G.A. & McMichael, A. (2015). Evolution of the immune system in humans from infancy to old age. Proceedings of the Royal Society B 282, 20143058.
- Stewart-Merrill, T.E. & Cáceres, C.E. (2018). Within-host complexity of a plankton-parasite interaction. *Ecology*, 99, 2864–2867.
- Stewart-Merrill, T.E., Rapti, Z. & Cáceres, C.E. (2021). Host controls of within-host disease dynamics: Insight from an invertebrate system. *Am. Nat.*, 198, 317–332.
- Stewart Merrill, T.E., Hall, S.R., Merrill, L. & Cáceres, C.E. (2019). Variation in immune defense shapes disease outcomes in laboratory and wild Daphnia. *Integr. Comp. Biol.*, 59, 1203–1219.
- Strauss, A.T., Hite, J.L., Civitello, D.J., Shocket, M.S., Cáceres, C.E. & Hall, S.R. (2019).
 Genotypic variation in parasite avoidance behaviour and other mechanistic, nonlinear components of transmission. Proceedings of the Royal Society B 286, 20192164.

(2016). Habitat, predators, and hosts regulate disease in Daphnia through direct and indirect pathways. *Ecol. Monogr.*, 86, 393–411.

Strauss, A.T., Shocket, M.S., Civitello, D.J., Hite, J.L., Penczykowski, R.M., Duffy, M.A., et al.

- Telfer, S., Birtles, R., Bennett, M., Lambin, X., Paterson, S. & Begon, M. (2008). Parasite interactions in natural populations: insights from longitudinal data. *Parasitology*, 135, 767–781.
- Tessier, A.J. & Woodruff, P. (2002). Trading off the ability to exploit rich versus poor food quality. *Ecol. Lett.*, 5, 685–692.
- Wale, N., Sim, D.G. & Read, A.F. (2017). A nutrient mediates intraspecific competition between rodent malaria parasites in vivo. Proceedings of the Royal Society B 284.
- Wilensky, U. (1999). Netlogo.

Figure Legends

Figure 1: Diagram of three ways that parasites can interact at the single-host scale (left panel), and age-mediated epidemiological feedback loops (right panel). Picture represents side view of

D. dentifera, where green lines represent host gastrointestinal tract, blue dots represent bacterial

spores, and thin lines represent fungal spores. (A) Parasites can alter the rate at which *Daphnia* feed, and thus the rate at which they contact further parasites (Strauss *et al.* 2019). (B) The probability that an ingested parasite will infect a *Daphnia* host is determined by the probably that the parasite can penetrate the gut wall and the host's immune response (Stewart Merrill *et al.* 2019; Izhar *et al.* 2020). Parasites can thus alter the host's susceptibility to one another if they alter the host immune response. (C) In successfully co-infected hosts, parasites can alter the number of inter-specific infectious spores released from *Daphnia* at death (Ben-Ami *et al.* 2011; Clay *et al.* 2019b), possibly by altering parasite growth rates, host lifespan, or host body size. In the right panel, the interactions shown at the individual scale (as shown in the left panel) determine parasite transmission rate, which determines average age of hosts at infection, which determines in turn how parasites interact at the individual host scale.

Figure 2: Age alters per spore infection probability, but this depends on whether the host was previously infected. X-axis shows host age, and Y-axis per spore probability of infection. Solid lines show linear regression of the mean, and bands show standard error. Note that the Y-axis scale is different between the panels because our bacterium generally has a much lower per spore infection probability than our fungus. No raw data points are shown as the per spore probability of infection was derived rather than directly measured.

Figure 3: Age and co-infection status interact to alter bacterial spore yield and have no effect on fungal spore yield. X-axis shows host age, and Y-axis shows number of infectious spores

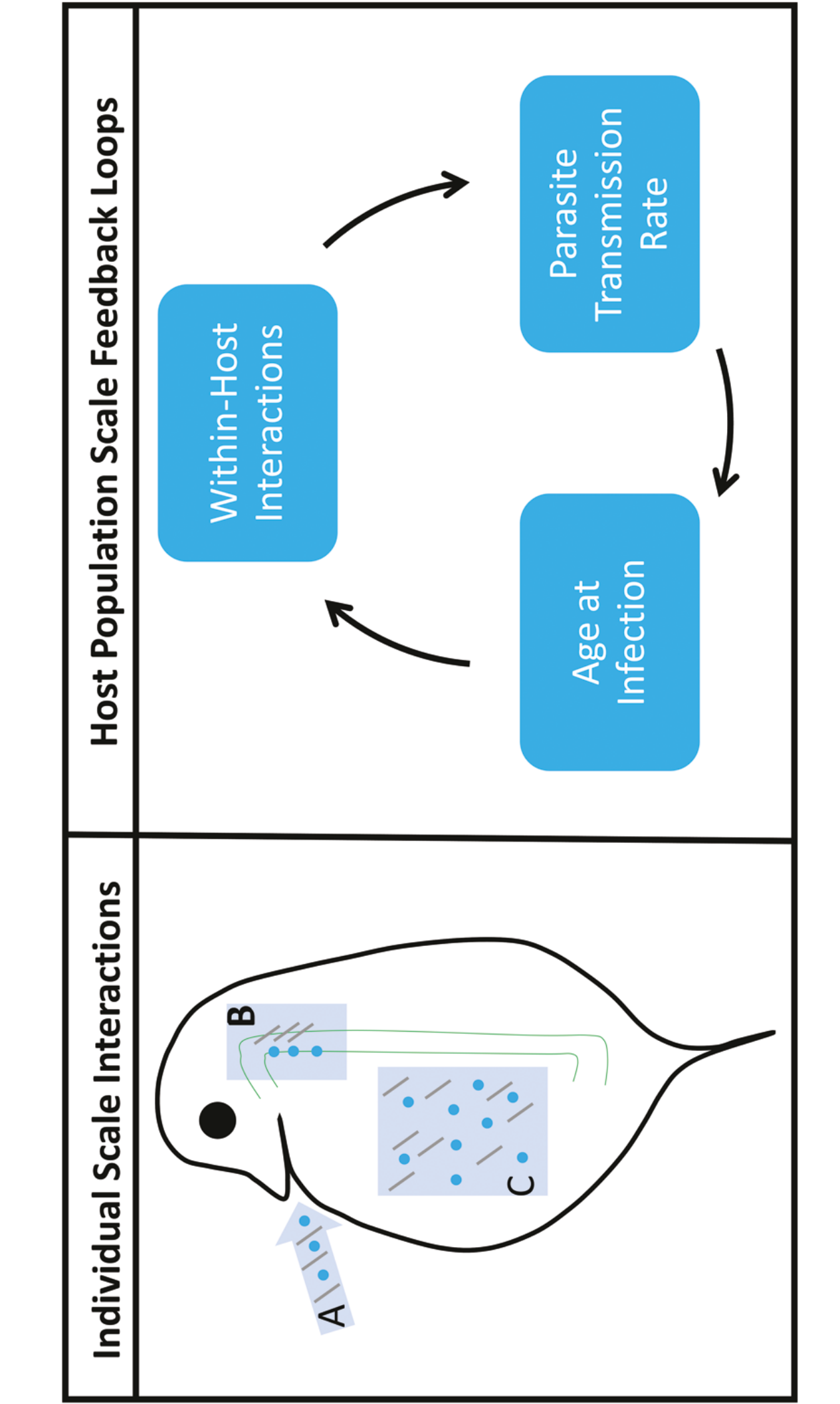
released from hosts at death. Points are raw measurements of individual spore yields, solid lines show best fitting linear model, and bands show standard error. For bacteria spore yield, lines represent different treatments, while for fungi spore yield, the line is the average of all treatments, as our linear model showed no significant impact of host age at infection or co-infection on spore yield.

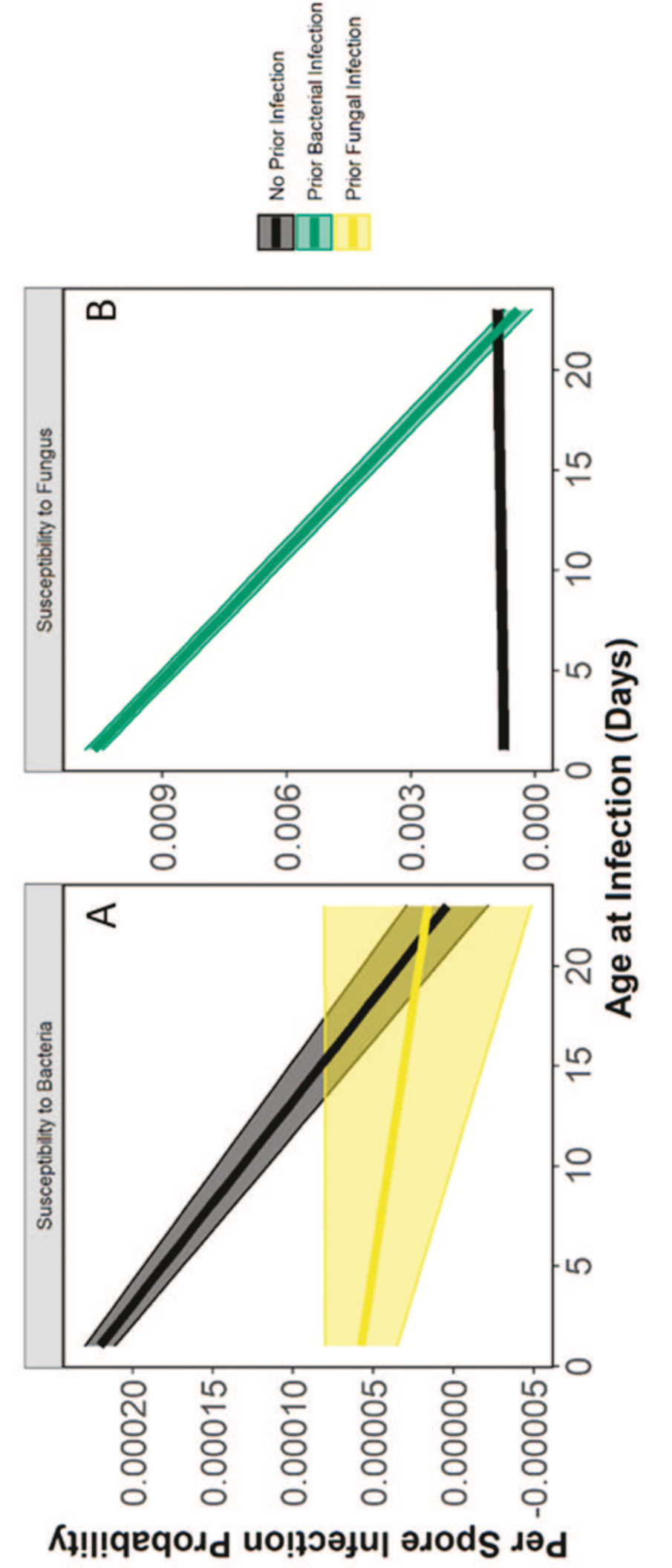
Figure 4: X-axis shows days of the epidemic, and Y-axis shows fungal or bacterial infection prevalence. Lines are means over 60 model runs, with bands that contain 95% of stochastic model outcomes. Thus, overlapping bands indicate that deterministic differences in prevalence due to parasite presence were smaller than the impact of stochastic variation on prevalence. Colors indicate which parasites were present in the population. Vertical bars indicate range of mean prevalence values over time over 95% of model runs. For these simulations, initial ages of individuals in a population were drawn from a normal distribution with a mean of either 10 or 24 days. Additionally, initial age at infection was set to either 4 or 24 days for infected individuals seeding the epidemic.

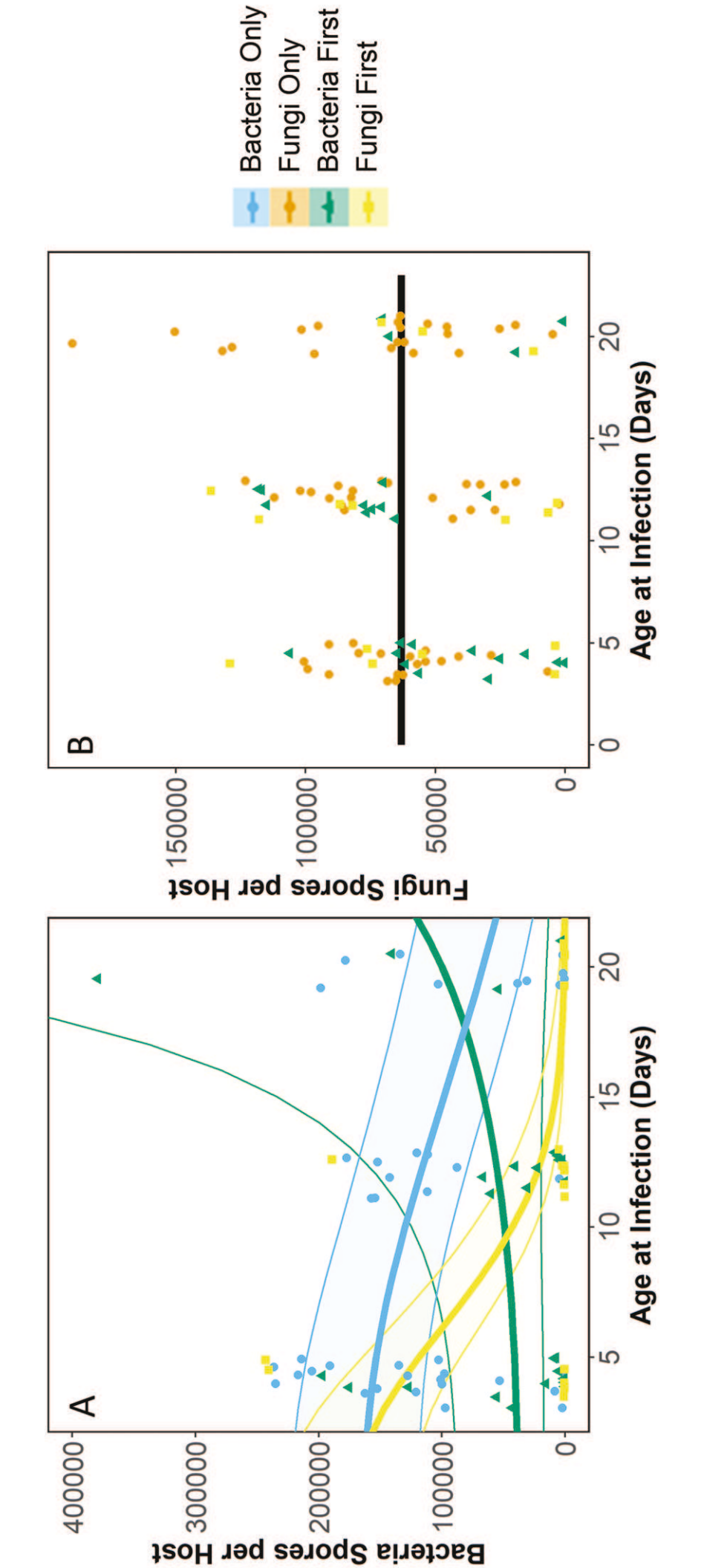
Figure 5: Variation in epidemiologically relevant parameters with age eliminates the effect of coinfection on epidemic dynamics. The Y-axis shows mean bacterial or fungal infection prevalence in singly- or co-infected populations over 60 model runs, over time on the X-axis. Panels with "Set age" indicate that host susceptibility, feeding rate, spore yield, and birth rate were constant for all hosts and were set based on a single host age (a) and age at infection (γ_i). In contrast, panels with "Age Varies" indicate that per spore susceptibility, feeding rate, spore yield, and birth rate were allowed to vary with host age and age at infection as measured in our laboratory experiment. Solid line indicates mean prevalence across model runs, while bands

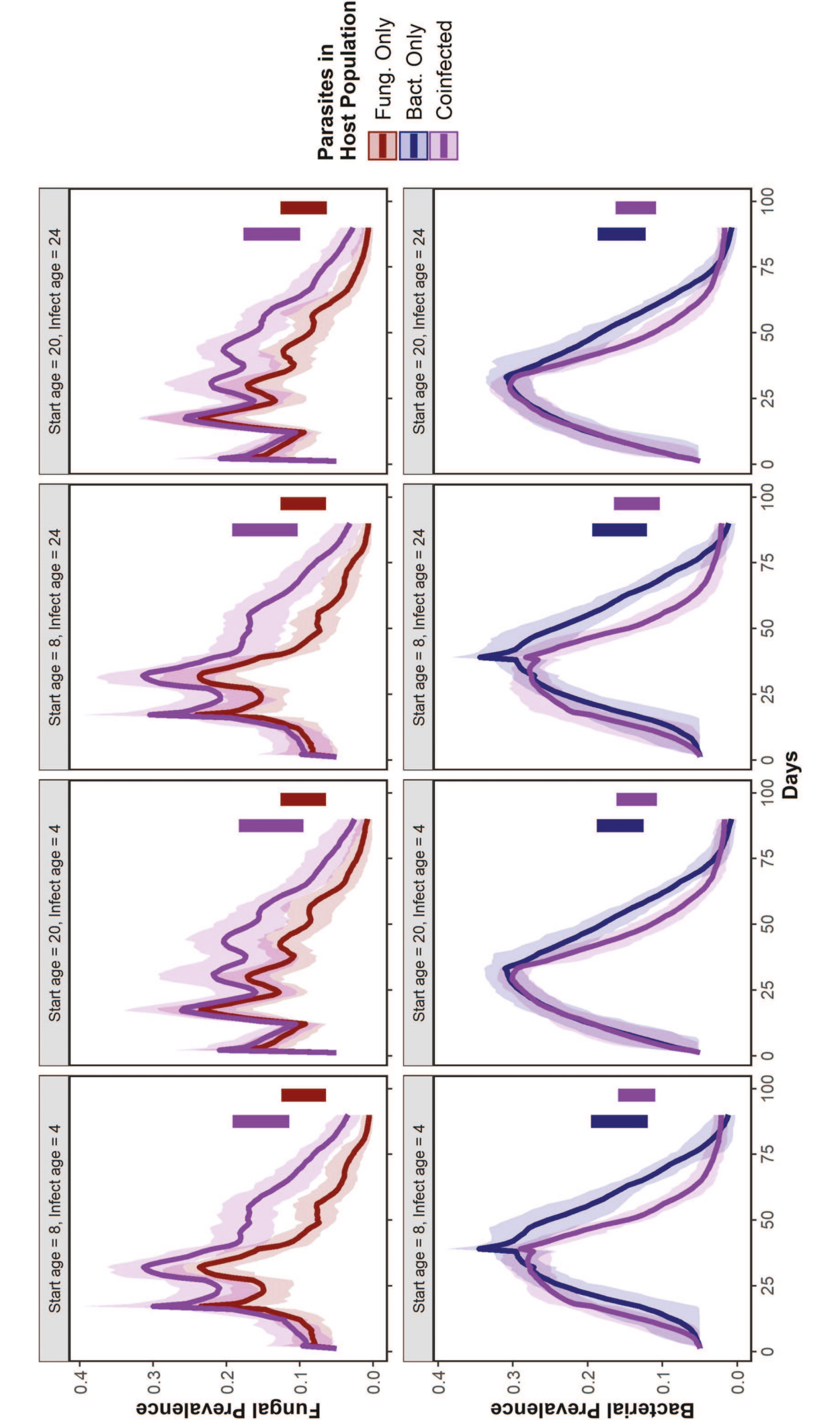
contain 95% of stochastic model outcomes. Vertical bars indicate range of mean prevalence values over time over 95% of model runs.

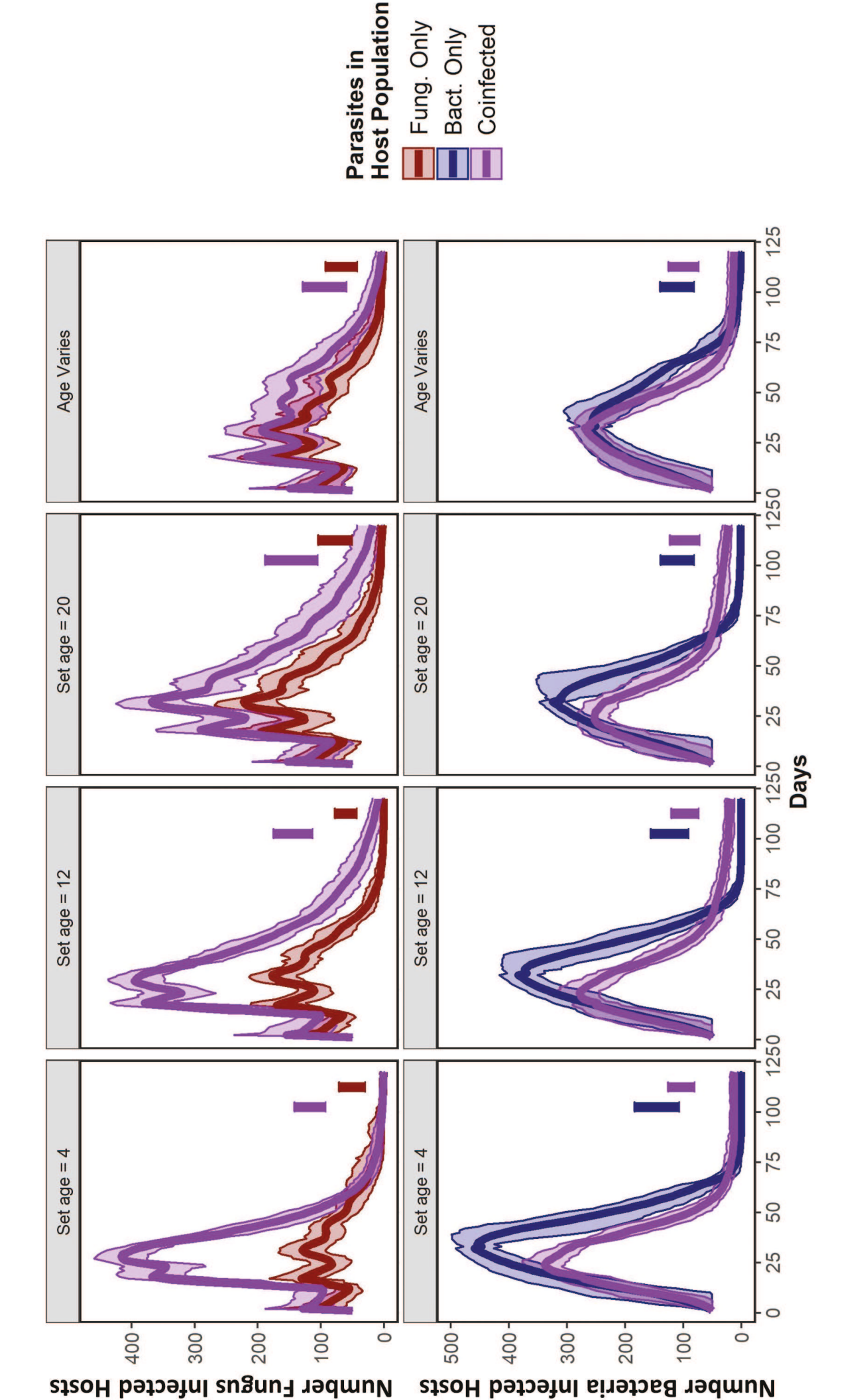
Figure 6: The probability of infection can fall off sharply as hosts age. The Y-axis shows the probability that a host will be infected after 24 hours of being exposed to a certain dosage of infectious propagules in the environment, given the host's feeding rate and per-spore infection probability. The X-axis indicates the age of the host. Panels A and B indicate infection probabilities by the fungi, panels C and D indicate infection probabilities by the bacteria. Panels A and C indicate infection probability with no prior infection or exposure to the other parasite, panels B and D indicate prior infection by the other parasite. Line color indicates relative spores per liter compared to the approximate maximum spores of the given parasite recorded during model runs of single parasite epidemics.

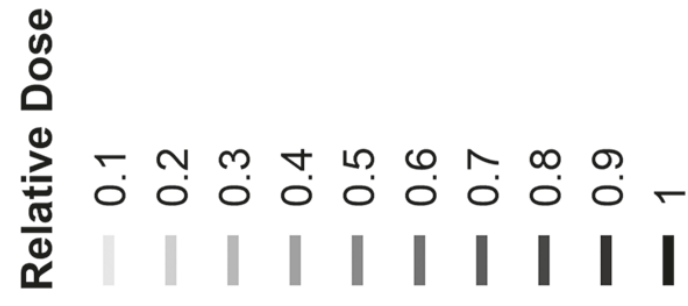


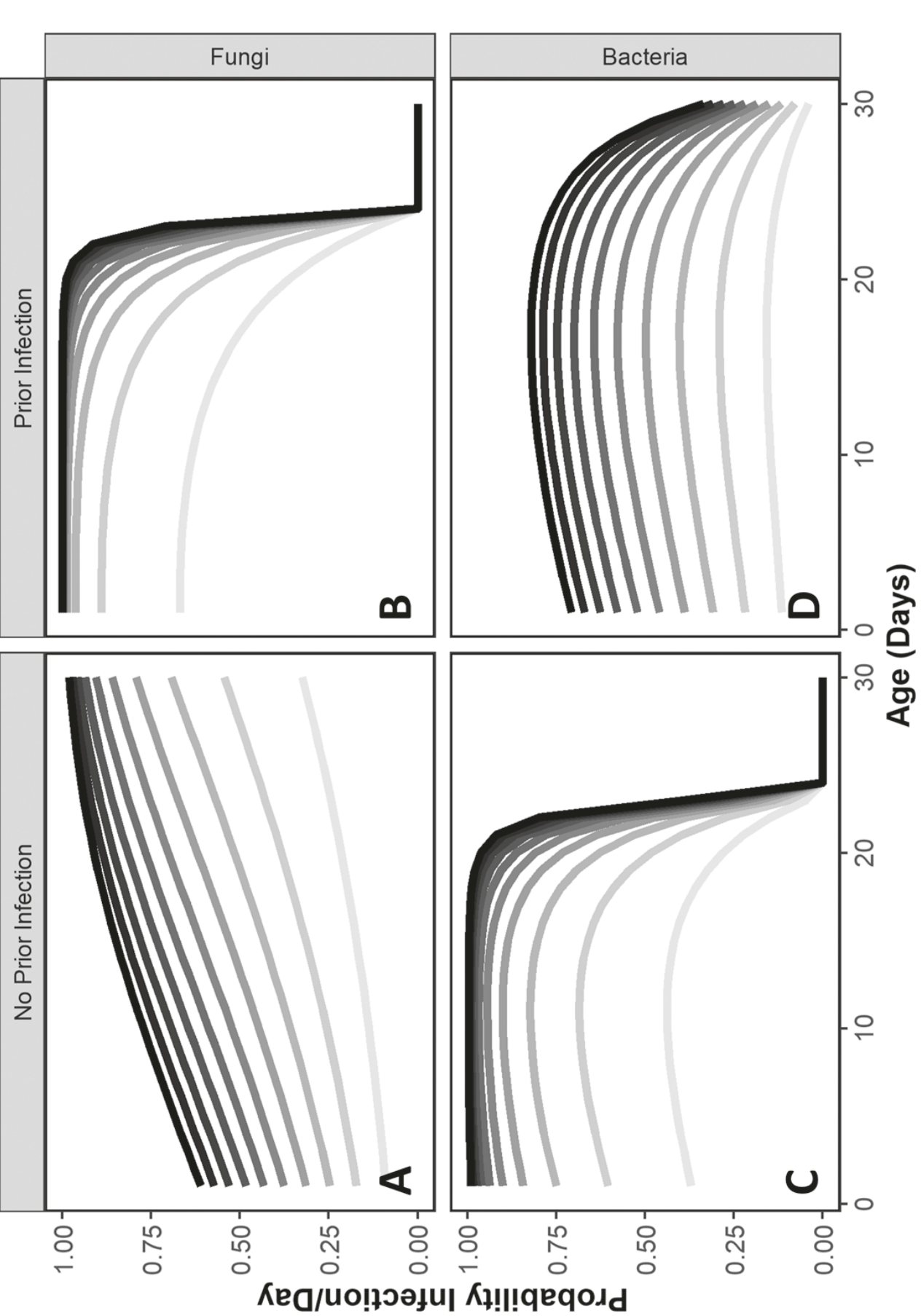












Supplementary materials for 'Age structure eliminates the impact of coinfection on epidemic dynamics in a freshwater zooplankton system'

Patrick A. Clay, ¹ Sabrina Gattis, ² Jade Garcia, ¹ Vincent Hernandez, ¹ Frida Ben-Ami, ² and Meghan A. Duffy ¹

The American Naturalist

¹ Department of Ecology & Evolutionary Biology, University of Michigan

² School of Zoology, George S. Wise Faculty of Life Sciences, Tel Aviv University, Tel Aviv 6997801, Israel

Study Design

Table S1: Infection schedule for each treatment. B and F indicate infection by the bacteria and the fungi, respectively. C indicates hosts exposed to ground up uninfected hosts as a control. f indicates feeding rate measurements.

Treatment	Day 4	Day 7	Day 10	Day 12	Day 15	Day 18	Day 20	Day 23	Day 26
1	C (f)	C (f)	C (f)	(f)	C (f)	C(f)	C (f)	C (f)	C (f)
2	B (f)	C (f)	С	С	С	С	С	С	С
3	F (f)	C (f)	С	С	С	С	С	С	С
4	B (f)	F (f)	C (f)	С	С	С	С	С	С
5	F (f)	B (f)	C (f)	С	С	С	С	С	С
6	С	С	С	B (f)	C (f)	С	С	С	С
7	С	С	С	F (f)	C (f)	С	С	С	С
8	С	С	С	B (f)	F (f)	C (f)	С	С	С
9	С	С	С	F (f)	B (f)	C (f)	С	С	С
10	С	С	С	С	С	С	B (f)	C (f)	С
11	С	С	С	С	С	С	F (f)	C (f)	С
12	С	С	С	С	С	С	B (f)	F (f)	C (f)
13	С	С	С	С	С	С	F (f)	B (f)	C (f)

Host Fitness

To parameterize an agent-based model of multi-parasite dynamics, we measured the impact of infection status and age at infection on host fitness. To measure host lifespan, we checked hosts

for death every day. To measure host fecundity, we moved hosts to clean tubes with fresh water every two days. While moving animals to their new tubes, we counted and discarded juveniles. For calculating host fitness in each treatment, we only included hosts that were successfully infected by all parasites to which they were exposed.

Total Host Fitness

Generally, parasites reduced lifetime reproduction of hosts. The reduction in lifetime reproduction due to infection was greater when hosts were infected at an earlier age, as this impacted a larger proportion of their reproductive timeline (p<0.001 in all treatments). We found no non-linear effects of age at first infection on fitness. If hosts were only infected with the bacteria and infection occurred late in the host's life (day 20), then infected hosts had a higher lifetime reproduction than unexposed hosts.

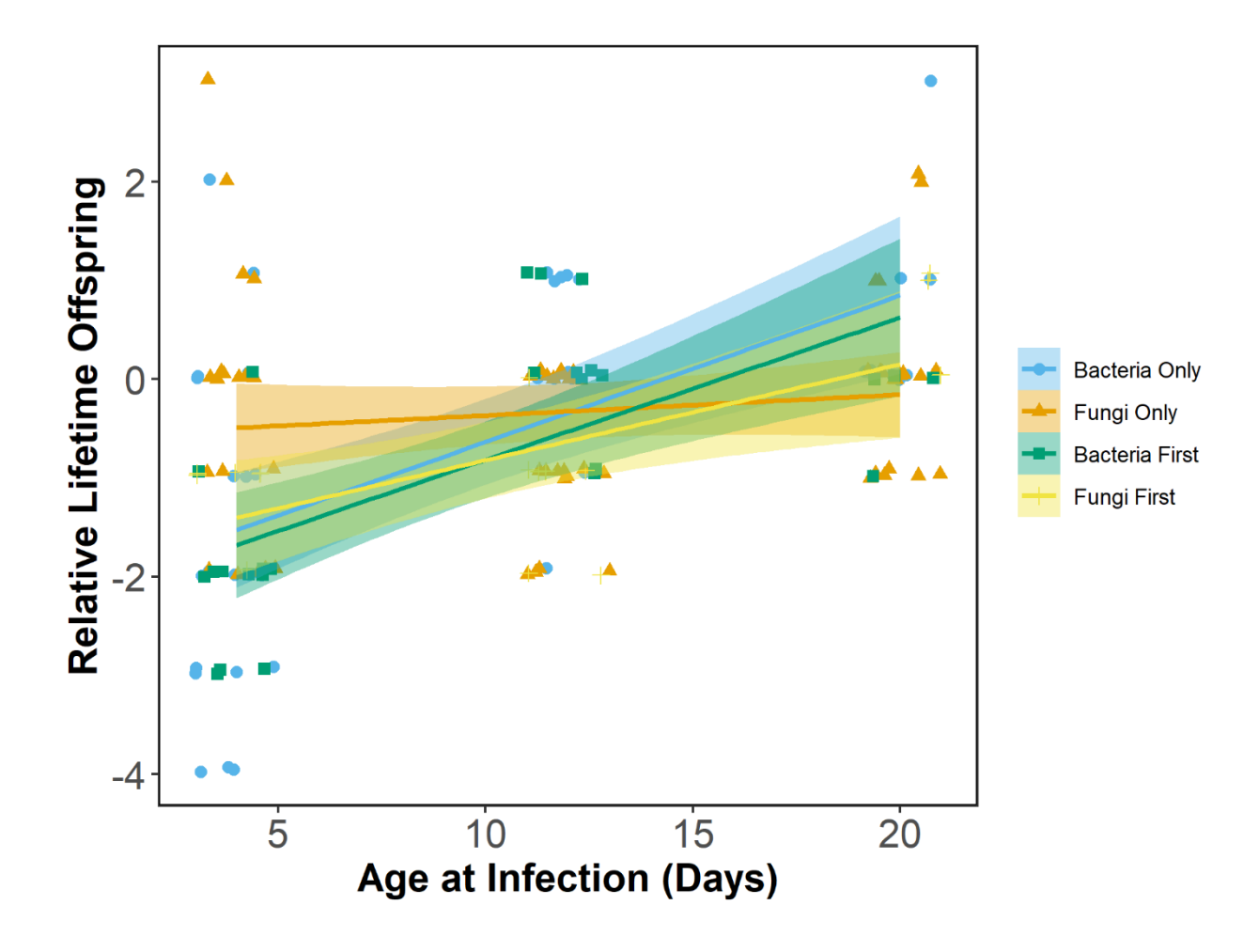


Figure S1: Infection reduces lifetime reproduction, but this effect is reduced if infection occurs late in host lifespan. Y-axis shows lifetime reproduction of infected hosts compared to the average lifetime reproduction of unexposed hosts. X-axis shows age at first infection. We only show data from hosts infected by all parasites to which they were exposed. Solid lines represent mean change in lifetime offspring due to single infection by the bacteria (blue), single infection by the fungi (orange), coinfection with the bacteria arriving first (green), and coinfection with the fungi arriving first (yellow). Bands represent 95% confidence intervals of the mean.

To parameterize our model, we examined the impact of age at infection on lifespan and births per day. Our fungal parasite has a larger impact on host lifespan than our bacterial parasite, which does not always alter host lifespan (Clay et al. 2018). Further, our fungal pathogen kills

hosts at a fairly constant time after host exposure. Thus, we first analyzed whether time until death after exposure to the fungi was altered by bacterial infection or age at exposure using the lm function in R. The model with the lowest AIC was the model with only time since infection as an explanatory variable (Table S2A). Hosts lived, on average, 16.3 days after fungal infection +/- standard error of 0.62 days (p<0.001). This did not change across any treatment, and death due to infection came before intrinsic mortality even in hosts infected late in life.

We then examined hosts infected only with the bacteria. The model with the lowest AIC was the model with only time since infection as an explanatory variable (Table S2B). For hosts infected only with the bacteria, host lifespan after infection was intercept of 31.4 days +/- 1.34 days (p<0.001).

See Table S3A and B for full lifespan model summary.

Table S2A: AIC values for models of post-infection time until death in hosts infected by the fungi (single or coinfections). Treatment indicates whether coinfection occurred and the order of infection. Age refers to the age of the host (in days) when infected by the fungus. We selected the intercept only model since it was the simplest model with $\Delta AIC < 2$.

Model	AIC	AAIC
Intercept only	674.3	0
Age	675.1	0.8
Age ²	675.9	1.6
Treatment	677.8	3.5
Age + Treatment	678.8	4.5
Age ² + Treatment	679.5	5.2

Age + Age ² + Treatment	676.3	2
Age + Treatment + Age *	680.3	6
Treatment		
$Age^2 + Treatment + Age^2 *$	680.2	5.9
Treatment		
Age + Age ² + Treatment +	678.6	4.3
Age * Treatment		
Age + Age ² + Treatment +	679.1	4.8
Age ² * Treatment		
Age + Age ² + Treatment +	681.4	7.1
Age * Treatment + Age ² *		
Treatment		

Table S2B: AIC values for models of post-infection time until death in hosts singly infected by the bacteria. Day refers to age (in days) at bacterial infection We selected the intercept only model since it was the simplest model with Δ AIC < 2.

Model	AIC	AAIC
Intercept only	302.3	0
Age	304.6	2.3
Age ²	303.7	1.4
$Age + Age^2$	304.0	1.7

Table S3A: Results of linear model testing how age at infection and coinfection altered post-infection time until death in hosts infected by the fungi. Degrees of freedom = 102.

Explanatory Var.	Category	P Value	Parameter	Value	Error
Life after fungal exposure intercept	Discrete	<2e-16	l_S	16.3 days	0.62

Table S3B: Results of linear model testing how age at infection altered post-infection time until death in hosts singly infected by the bacteria. Degrees of freedom = 41.

Explanatory Var.	Category	P Value	Parameter	Value	Error
Life after bacterial exposure intercept	Discrete	<2e-16	l_S	31.4 days	1.34

Births per day: Prior evidence suggests that the parasites in our study change host fecundity over time, but do not immediately impact fecundity upon exposure (supplemental information of Clay et al. 2018). Thus, we ran a linear model for offspring per day using age and time since infection for each infection treatment as explanatory variables. The model with the lowest AIC included host age, host age squared, and treatment, but no interaction terms (Table S4). Analyzing the births per day of unexposed hosts for the length of the experiment, and infected hosts after they became infected, we see that offspring per day of all hosts decrease with host age (p<0.001) and increase with host age squared (p<0.001). Additionally, the offspring per day of all infected hosts decrease with time since infection, though this result is non-significant for hosts singly infected by the fungus (p = 0.121, Table S5). Incorporating all terms from the model with the lowest AIC, the offspring per day, (b), of hosts in our model is calculated as

$$b = b_{int} + b_{slope}a + b_{slope,2}a^2 + b_{B,slope}(a - \gamma_B)I_B + b_{F,slope}(a - \gamma_F)I_F$$

$$+ b_{BF,slope}(a - \gamma_F)I_{BF} + b_{FB,slope}(a - \gamma_B)I_{FB} \quad eq. S2$$

See Table S5 for full birthrate model summary.

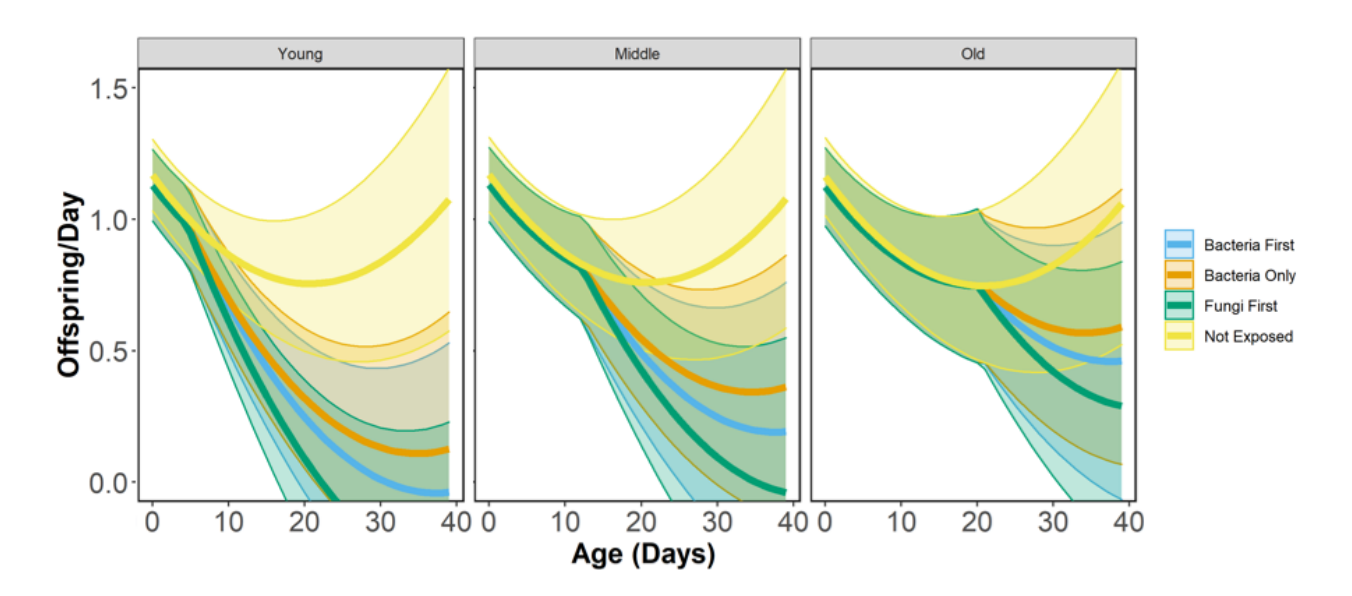


Figure S2: Infection reduces offspring/day. Y-axis shows lifetime offspring/day. X-axis shows age of hosts. Solid lines represent results from linear regression for offspring of hosts infected by the bacteria, coinfected with the bacteria arriving first, coinfected with the fungi arriving first, and unexposed hosts. Bands represent standard error. We do not show regression results for hosts only infected by the fungi, as they did not significantly differ from unexposed hosts.

Table S4: AIC values of models for births per day. In this instance, "Treatment" is a combined variable of both which parasites had infected the host, the order of infection, and time since infection. We selected the Age + Age² + Treatment model since it was the simplest model with Δ AIC < 2.

Model	AIC	AAIC
Intercept Only	7022	91
Age	7021	90

Age ²	7016	85
Treatment	6983	52
$Age + Age^2$	7001	76
Age + Treatment	6951	26
Age ² + Treatment	6936	11
Age + Age ² + Treatment	6925	0
Age + Treatment + Age *	6936	11
Treatment		
Age ² + Treatment + Age ² *	6929	4
Treatment		
Age+ Age ² + Treatment +	6926	1
Age * Treatment		
Age+ Age ² + Treatment +	6926	1
Age ² * Treatment		

Table S5: Results of generalized linear model testing how host age, and time since various infection treatments, altered offspring per day. Degrees of freedom = 2160.

Explanatory Var.	Category	P Value	Parameter	Value	Error
Intercept	Discrete	3.11e-16	b_{int}	1.16 offspring/day	0.141
Age	Continuous	0.000231	b_{slope}	-0.0397 offspring/day ²	0.0108
Age ²	Continuous	8.92e-08	$b_{slope,2}$	0.000958 offspring/day ³	0.000179
Days since single bacterial infection	Continuous	8.46e-16	$b_{B,slope}$	-0.0263 offspring/day ²	0.00324

Days since single fungal infection	Continuous	0.121	$b_{F,slope}$	-0.00843 offspring/ day ²	0.00543
Days since coinfection, bacteria first	Continuous	6.91e-07	$b_{BF,slope}$	-0.0326 offspring/day ²	0.00654
Days since coinfection, fungi first	Continuous	4.83e-06	$b_{FB,slope}$	-0.0417 offspring/day ²	0.00909

Full Presentation of Model significance for feeding rate, host susceptibility, and spore yield

The following tables are described and referenced in the main text.

Table S6: AIC Values for models of host feeding rate. In this instance, "Treatment" is a combined variable of which parasites had infected the host and the order of infection. We selected the Age + Treatment + Age * Treatment model since it was the simplest model with $\Delta AIC < 2$. We did not include quadratic age terms as we had to discard feeding measurements from middle-aged hosts.

Model	AIC	ΔAIC
Intercept Only	762.9	315.8
Age	481.9	34.8
Treatment	741.2	294.1
Age + Treatment	467.9	20.8
Age + Treatment + Age *	447.1	0
Treatment		

Table S7: Results of generalized linear model testing how host age, presence of bacterial or fungal spores in the environment, and prior infection with the fungi or the bacteria altered host feeding rate. We found that neither spore exposure nor prior infection altered host feeding rate. Thus, we removed parasite factors as an explanatory variable when estimating parameter values for our agent-based model (Table S5). We note that our experiment differed from others that did find effects of infection on feeding rate, in that ours measured effects of infection on feeding rate while exposed to other pathogens, and found no effect, while other studies (Penczykowski et al. 2022) found that infection decreased host feeding rate in the absence of infectious spores. This suggests either (a) possible interactions between infection status and environmental spore density on host feeding rate, or (b) genotype by genotype interactions that could be explored in future studies. These results are from glm with a Gamma distribution and a log link function. Degrees of freedom = 385.

Explanatory Var.	P value	Parameter	Estimate	Error
Intercept	8.24e-05	f _{int}	-0.650 ml/hour	0.1650924
Host Age	5.2e-07	f_{slope}	0.0527 ml/hour/da	0.0105084
Exposure to Bacteria	0.297	f_B	-0.257 ml/hour	0.2469109
Exposure to Fungi	0.886	f_F	-0.0334 ml/hour	0.2383736
Exposure to Bacteria after Fungal Infection	0.579	f_{FB}	-0.223 ml/hour	0.4019567
Exposure to Fungi after Bacterial Infection	0.623	f_{BF}	-0.236 ml/hour	0.4809959
Age * Exposure to Bacteria	0.0789	$f_{slope,B}$	0.0286 ml/hour/da y	0.0162525

Age * Exposure to Fungi	0.457	$f_{slope,F}$	-0.0118 ml/hour/d	0.0159307
			ay	
Age * Exposure to Bacteria after	0.540	$f_{slope,FB}$	0.0150 ml/hour/da	0.0245076
Fungal Infection			У	
Age * Exposure to Fungi after	0.982	$f_{slope,BF}$	-0.00751 ml/hour/	0.0329695
Bacterial Infection			day	

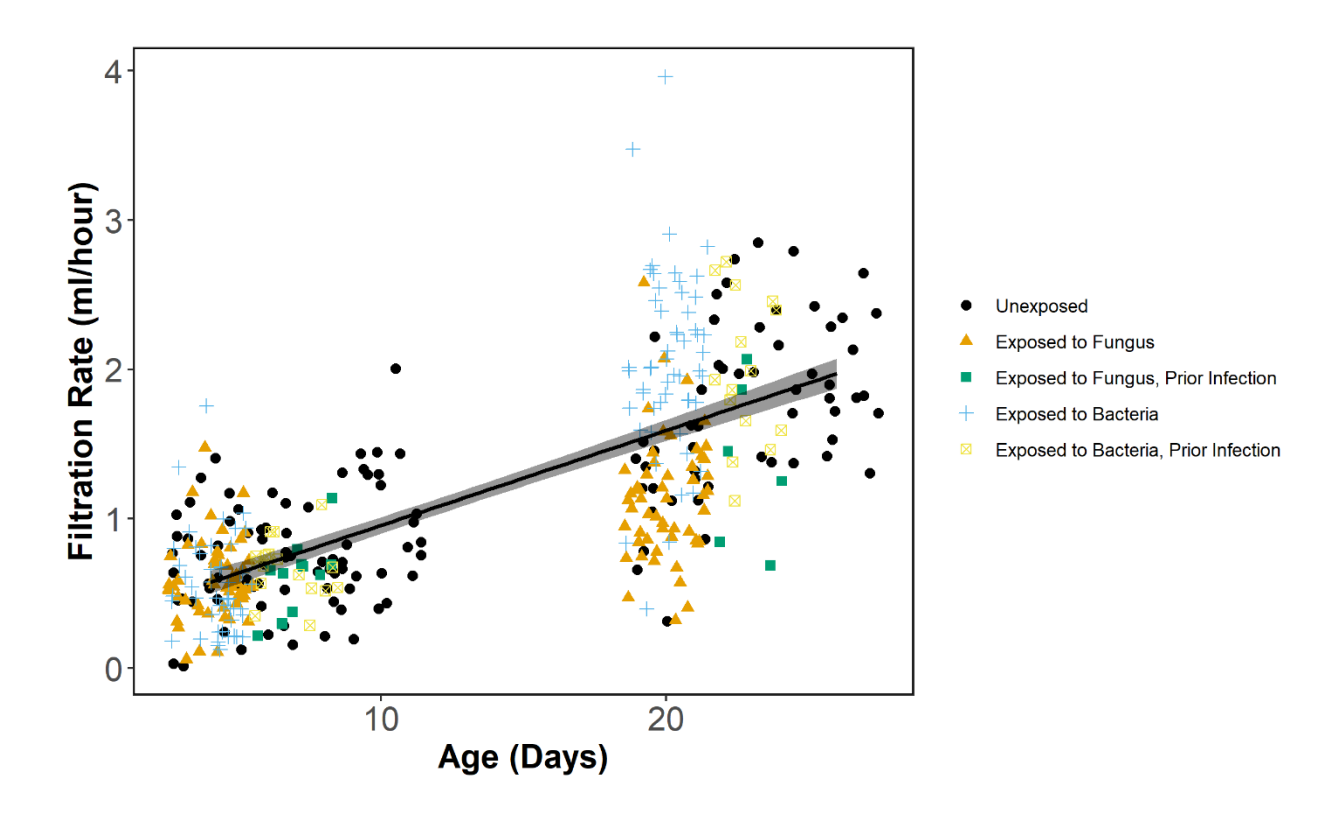


Figure S3: GLMs found no significant results of exposure treatment or infection status on feeding rate. The X-axis shows the age of the hosts, while the Y-axis shows the feeding rate in ml of water filtered per hour. Points show individual feeding rates with colors and shapes indicating various treatments, while line and band show linear model fit and 95% confidence

interval, only using age as an explanatory variable, given that it was the only significant parameter.

Table S8: AIC Values for models of per spore bacterial infectivity. We selected the Age + Prior Fungal Infection + Age * Prior Fungal Infection model since it was the simplest model with Δ AIC < 2. We did not include quadratic age terms as we had to discard feeding measurements from middle-aged hosts.

Model	AIC	ΔΑΙC
Intercept	734.3	594.4
Age	736.3	596.4
Prior fungal Infection	584.4	444.5
Age + Prior Fungal Infection	380.3	240.4
Age + Prior Fungal Infection	139.9	0
+ Age * Prior Fungal		
Infection		

Table S9: Maximum likelihood estimates for how bacterial per-spore infectivity changed with host age, prior fungal infection, and the interaction between the two factors. Additionally, we show accompanying agent-based model parameterization.

Explanatory Var.	Category	P Value	Parameter	Value	Error
Intercept	Discrete	< 2e-16	$\mu_{B,int}$	2.3029e-04	8.61e-06
Age	Continuous	< 2e-16	$\mu_{B,a}$	-9.8447e-06	7.30e-07
Prior Fungal Infection	Categorical	< 2e-16	$\mu_{F.prior}$	-1.7102e-04	1.20e-05
Age * Prior Fungal Infection	Continuous	1.562e-11	$\mu_{F.prior,a}$	7.9537e-06	1.18e-06

Table S10: AIC Values for models of per spore fungal infectivity. We selected the Age + Prior Bacterial Infection + Age * Prior Bacterial Infection model since it was the simplest model with Δ AIC < 2. We did not include quadratic age terms as we had to discard feeding measurements from middle-aged hosts.

Model	AIC	ΔΑΙC
Intercept	444.2	356.2
Age	446.2	358.2
Prior fungal Infection	197.6	109.6
Age + Prior Bacterial	199.6	111.6
Infection		
Age + Prior Bacterial	88.0	0
Infection + Age * Prior		
Bacterial Infection		

Table S11: Maximum likelihood estimates for how fungal per-spore infectivity changed with host age, prior bacterial infection, and the interaction between the two factors. Additionally, we show accompanying agent-based model parameterization.

Explanatory Var.	Category	P Value	Parameter	Value	Error
Intercept	Discrete	5.04e-13	$\mu_{F,int}$	7.41e-04	1.03e-04
Age	Continuous	< 2e-16	$\mu_{F,a}$	7.03e-06	1.64e-07
Prior Bacterial Infection	Categorical	< 2e-16	$\mu_{B.prior}$	1.04e-02	1.05e-04

Age * Prior	Continuous	< 2e-16	$\mu_{B.prior,a}$	-4.72e-04	4.76e-06
Bacterial Infection			. ,		

Table S12: AIC Values for models of bacterial spore yield. We selected the $Age^2 + Treatment + Age^2 *$ Treatment model since it was the simplest model with $\Delta AIC < 2$.

Model	AIC	ΔΑΙС
Intercept	2029	14
Age	2029	14
Age ²	2030	15
Treatment	2025	10
$Age + Age^2$	2030	15
Age + Treatment	2026	11
Age ² + Treatment	2026	11
Age + Age ² + Treatment	2026	11
Age + Treatment + Age *	2019	4
Treatment		
Age ² + Treatment + Age ² *	2015	0
Treatment		
Age+ Age ² + Treatment +	2021	6
Age * Treatment		
Age+ Age ² + Treatment +	2017	2
Age ² * Treatment		

Table S13: Results of generalized linear model testing how age at bacterial infection and coinfection status altered bacterial spore yield from infected hosts. Additionally, we show accompanying agent-based model parameterization. These results are from glm with a Gamma distribution and a log link function. Degrees of freedom = 78.

Explanatory	Category	P Value	Parameter	Estimate	Error
Var.					
Intercept	Discrete	<2e-16	$eta_{B,int}$	12.0	0.209
Age ²	Continuous	0.0265	$\beta_{B,a}$	-0.00222	0.00100
Coinfection: Bacteria First	Categorical	2.62e-05	eta_{B1}	-1.44	0.341
Coinfection: Fungi First	Categorical	0.7832	eta_{B2}	-0.116	0.420
Age ² * Coinfection: Bacteria First	Continuous	0.0116	$eta_{B1,a}$	0.00454	0.00180
Age ² * Coinfection: Fungi First	Continuous	4.03e-08	$eta_{B2,a}$	-0.0115	0.00210

Table S14: AIC Values for models of fungal spore yield. We selected the intercept only model since it was the simplest model with $\Delta AIC < 2$.

Model	AIC	ΔΑΙС
Intercept	2464	0
Age	2464	0

T	1 .
	1
2466	2
2465	1
2467	3
2467	3
2467	3
2470	6
2470	6
2471	7
2470	6
	2465 2467 2467 2467 2470 2470

Table S15: Results of generalized linear model to estimate fungal spore yield for our agent-based model.

Degrees of freedom = 102.

Explanatory Var.	Category	P Value	Parameter	Value	Error
Intercept	Discrete	< 2e-16	$eta_{F,int}$	63900	3670

Total Pathogen Fitness

Bacterial Success

In addition to examining the mechanistic components of parasite interactions, we examine the cumulative impact of host age and coinfection on parasite success. We define parasite success as the expected infectious spore yield from exposed hosts when considering both probability of infection and spore yield from infected hosts. In single infections, bacterial spore yield did not change with age at infection (p=0.538). If the bacteria arrived first in coinfected hosts, coinfection reduced bacterial spore yield at the intercept (-90% of spores, p<0.046), but again did not change with age at infection (p=0.122; compare blue and green symbols and lines in left panel of Figure 3). If the fungi arrived first in coinfected hosts, coinfection did not change bacteria spore yield at the intercept (p=0.774), but the decrease in spores with age at infection was greater (-21% of spores/days lived, p=0.00517; compare blue and yellow symbols and lines in the left panel of Figure 3; also see Figure S3 and Table S11 for all statistical results).

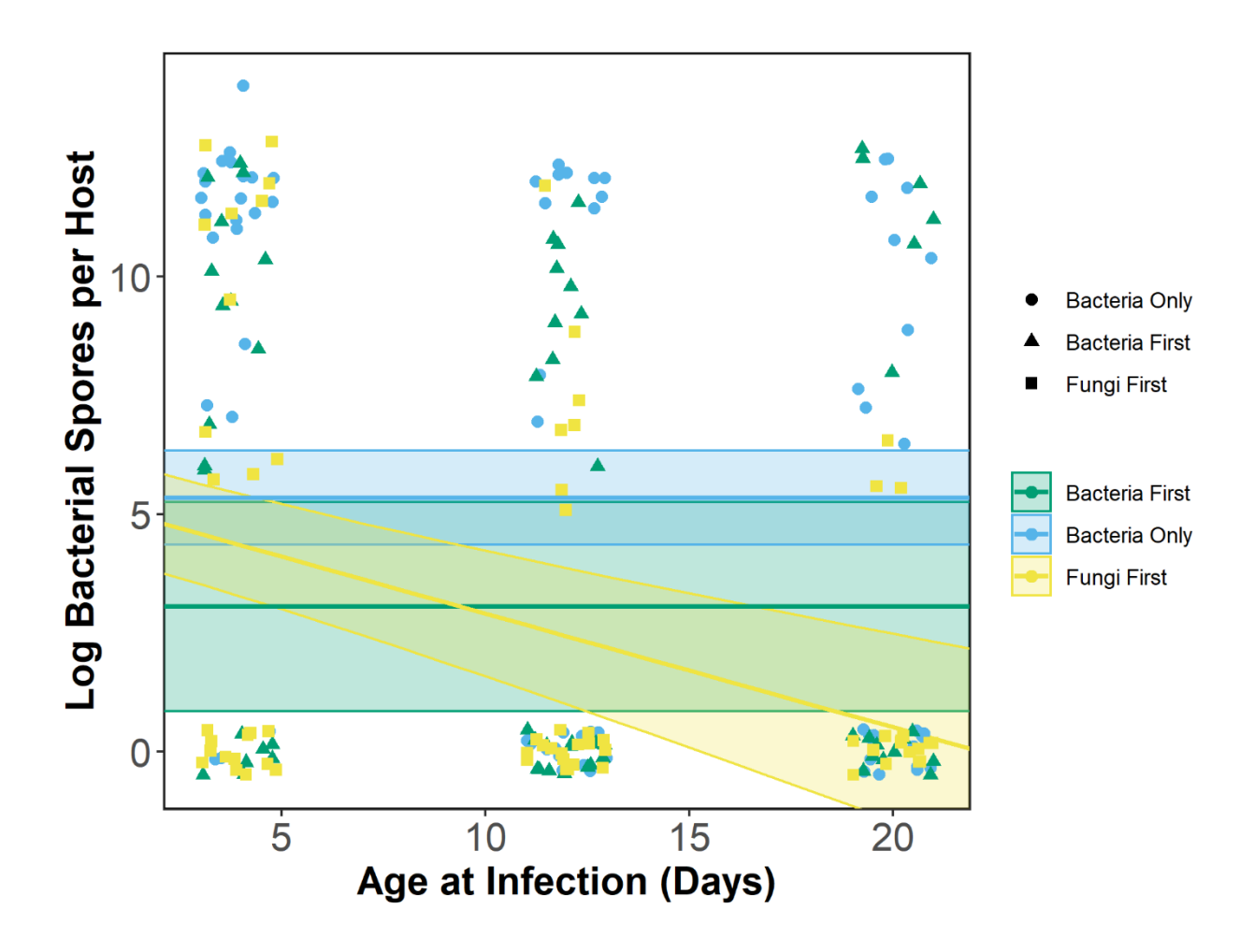


Figure S4: Age decreases bacterial success, but this depends on coinfection status. The Y-axis shows the log number of bacterial spores released from all hosts that were exposed to the bacteria, including hosts the bacteria did not infect. (We do not include hosts that were exposed to, but did not become infected by, the fungi). The X-axis shows host age when exposed to the bacteria (jittered to avoid point overlap). Solid lines are results of glm fit to a negative binomial distribution with bands representing standard error of the mean. Points represent individual spore yields.

Table S16: Results of generalized linear model on the impact of age at infection and infection status (singly infected, coinfected with the bacteria arriving first, coinfected with the fungi arriving first) on

bacterial success (the expected number of infectious spores released from a *Daphnia* exposed to the bacteria, considering both likelihood of infection, and spore yield from infected hosts). These results are from a glm with a negative binomial distribution and a log link function. Degrees of freedom = 93.

Explanatory Var.	P Value	Estimate	Error
Intercept	3.56e-07	5.32	1.04
Age	0.538	-0.110	0.180
Age Squared	0.959	0.000363	0.00712
Coinfection: Bacteria First	0.046	-2.25	1.13
Coinfection: Fungi First	0.774	0.312	1.09
Age * Coinfection: Bacteria First	0.122	0.130	0.0839
Age * Coinfection: Fungi First	0.00517	-0.239	0.0854

Fungal Success

We now ask: given exposure to the fungi, what is the expected infectious spore yield from that host if we consider both probability of infection and spore yield from infected hosts? In singly infected hosts, fungal success changes non-linearly with age at infection. Age at infection increases expected spore yield (+11% spores/day, p<0.0001) in a decelerating manner (-0.38% spores/day², p<0.0001), to create a humped relationship. In coinfected hosts where the bacteria arrived first, fungal spore yield was higher at the intercept (+31% spores) but increased less with age at infection (-6.6% of spores/day). In coinfected hosts where the fungi arrived first, fungal spore yield had the same intercept as in singly infected hosts (p=0.361), but again decreased less with age (+10% spores/day, p=0.0916, Figure S4, see Table S12 for all statistical results).

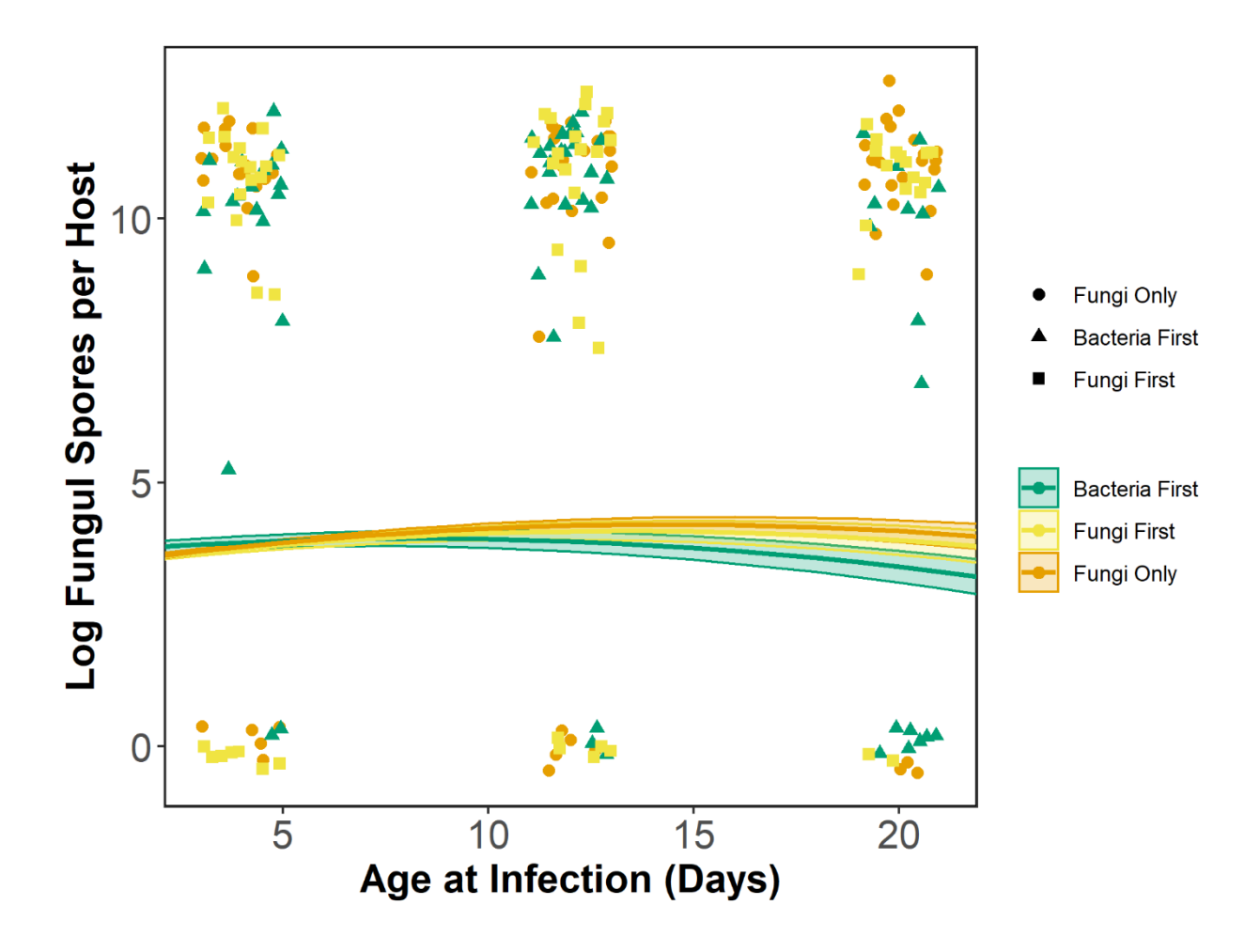


Figure S5: Age changes fungal spore yield in a humped shape manner. The Y-axis shows the log number of fungal spores released from all hosts that were exposed to fungi, including hosts the fungi did not infect. (We do not include hosts that were exposed to, but not infected by, bacteria). The X-axis shows host age when exposed to the fungi (jittered to avoid point overlap). Solid lines are results of glm fit to a negative binomial distribution with bands representing standard error of the mean. Points represent individual spore yields.

Table S17: Results of generalized linear model on the impact of age at infection and infection status (singly infected, coinfected with the bacteria arriving first, coinfected with the fungi arriving first) on

fungal success (the expected number of infectious spores released from a *Daphnia* exposed to the fungi, considering both likelihood of infection, and spore yield from infected hosts). Degrees of Freedom = 199.

Explanatory Var.	P Value	Estimate	Error
Intercept	< 2e-16	3.403	0.0502
Age	< 2e-16	0.111	0.00811
Age Squared	< 2e-16	-0.00387	0.000315
Coinfection: Bacteria First	7.64e-07	0.271	0.0548
Coinfection: Fungi First	0.361	0.0470	0.0515
Age * Coinfection: Bacteria First	< 2e-16	-0.0469	0.00426
Age * Coinfection: Fungi First	0.0196	-0.00891	0.00382

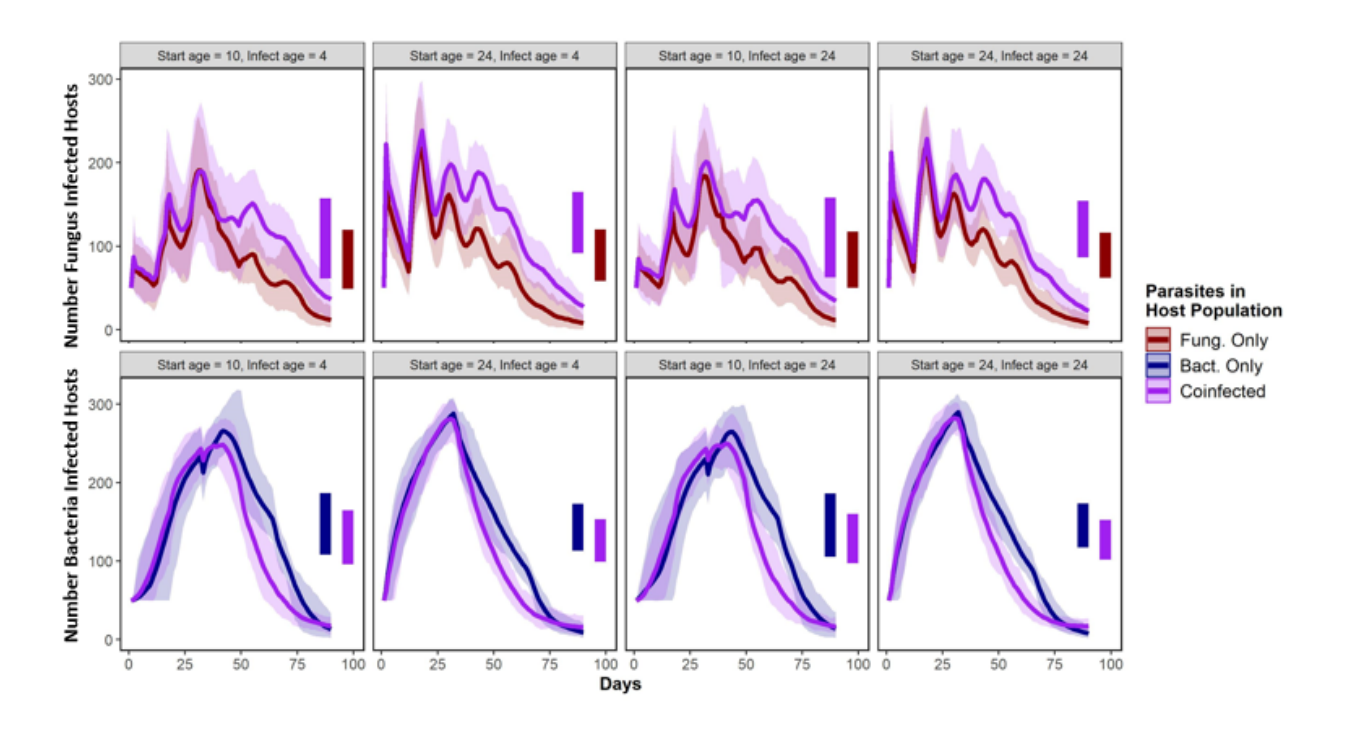


Figure S6: X-axis shows days of the epidemic, and Y-axis shows number of hosts infected by either the fungus or the bacteria. Lines are means over 60 model runs, with bands contain 95% of

stochastic model outcomes. Colors indicate which parasites were present in the population. Vertical bars indicate range of mean host density values over time over 95% of model runs. For these simulations, initial ages of individuals in a population were drawn from a normal distribution with a mean of either 10 or 24 days. Additionally, initial age at infection was set to either 4 or 24 days for infected individuals seeding the epidemic; an individual that was randomly designated as infected and that was, for example, 21 days old at the start of a simulation with an initial age at infection of 4 days would therefore be 21 days old and 17 days post-infection at the start of the simulation. After that first time step, age at infection was allowed to vary naturally. In these simulations, epidemiologically relevant parameters (feeding rate, perspore susceptibility, spore yield, and births per day) varied with host age.

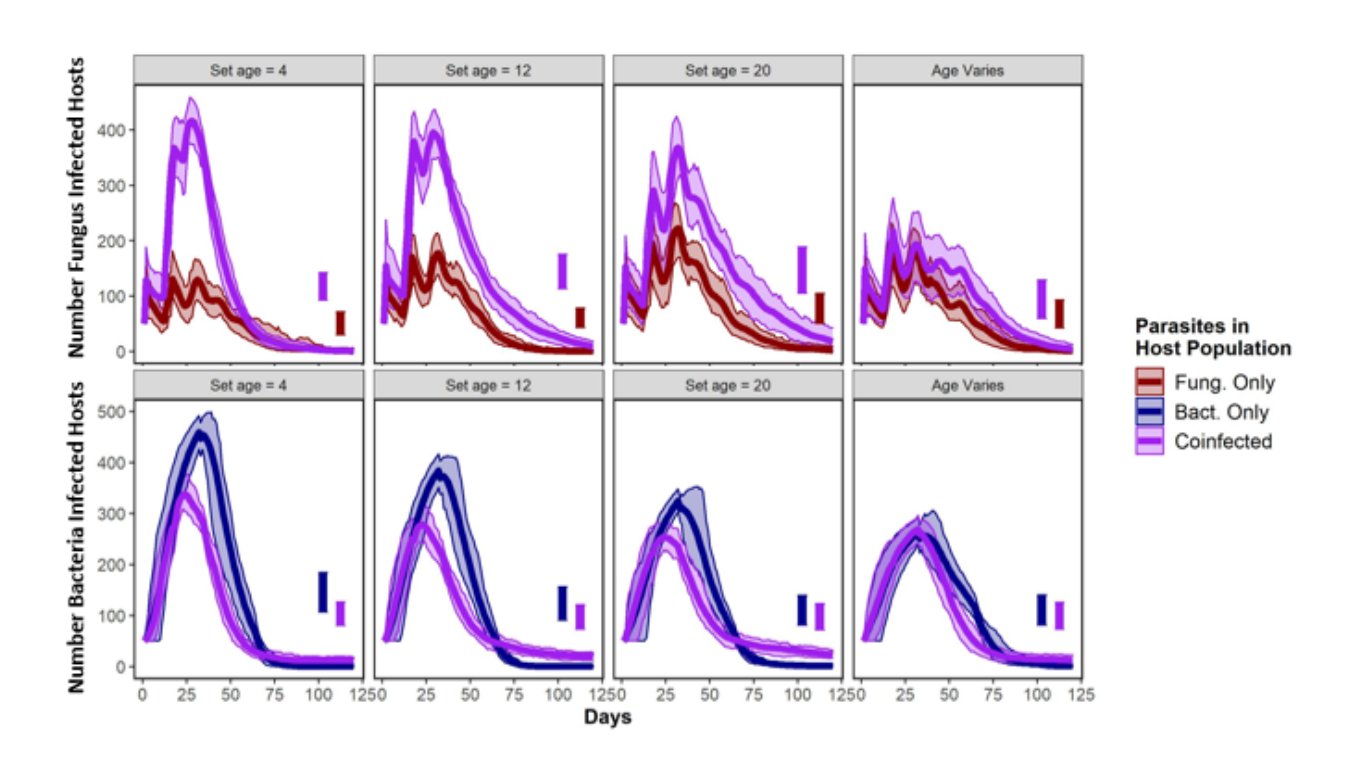


Figure S7: Mean age at infection and variation in age at infection alters density of infected hosts. The Y-axis shows number of hosts in the population infected with either the bacteria or the

fungus in singly- or co-infected populations over 60 model runs, over time on the X-axis. Panels with "Set age" indicate that host age (a) and age at infection (γ_i) were held constant for the purposes of calculating host susceptibility, feeding rate, and spore yield, while panels with "Age Varies" indicate that host age and age at infection were allowed to vary naturally; in these simulations, epidemiologically relevant parameters (feeding rate, per-spore susceptibility, spore yield, and births per day) varied with host age. Solid line indicates mean values across model runs, while bands contain 95% of stochastic model outcomes. Vertical bars indicate range of mean host density values over time over 95% of model runs.